REMOVAL OF PHENOL AND CADMIUM FROM CONTAMINATED WATER BY POLYMERIC MODIFIED GRAPHENE NANOMATERIALS

BY

ABIDEEN OJO SALAWUDEEN

A Thesis Presented to the
DEANSHIP OF GRADUATE STUDIES

KING FAHD UNIVERSITY OF PETROLEUM & MINERALS
DHAHRAN, SAUDI ARABIA

In Partial Fulfillment of the
Requirements for the Degree of

MASTER OF SCIENCE

In

ENVIRONMENTAL SCIENCES

DECEMBER, 2018

KING FAHD UNIVERSITY OF PETROLEUM & MINERALS

DHAHRAN- 31261, SAUDI ARABIA

DEANSHIP OF GRADUATE STUDIES

This thesis, written by **ABIDEEN OJO SALAWUDEEN** under the direction of his thesis advisor and approved by his thesis committee, has been presented and accepted by the Dean of Graduate Studies, in partial fulfillment of the requirements for the degree of **MASTER OF SCIENCE IN ENVIRONMENTAL SCIENCES.**

Dr. Abdullatif Al-Shuhail
Department Chairman

B. S. Tawabini 27/3/19
Dr. Bassam S. Tawabini
(Advisor)

Dr. Salam A. Zummo
Dean of Graduate Studies

عمادة الدراسات العليا
DEANSHIP OF GRADUATE STUDIES

Dr. Tawfik Abdo Saleh
(Member)

7/4/19
Date

Dr. Abdulaziz Al-Shaibani
(Member)

Dedicated to my lovely and supporting parents and family

ACKNOWLEDGMENTS

All sincere praises and unadulterated adorations are due to the Almighty Allah, the Lord of the worlds that made the completion of the research successful.

I appreciate King Fahd University of Petroleum and Minerals (KFUPM) for the admission opportunity as well as conducive learning and research environment. Also, I am grateful to the Ministry of Higher Education, Kingdom of Saudi Arabia for granting the scholarship.

As research is a team work, I really appreciate the support, patience, guidance and constructive criticism of my respected advisor, Dr. Bassam Tawabini. Also, special thanks Dr. Tawfik Saleh as well as Dr. Abdulaziz Al-Shaibani for their perseverance, support and guidance.

I also really appreciate the assistance of all the laboratory technicians who made the instrumental analyses achievable. The list includes but not limited to Mr. Tajudeen Oyehan, Mr. Eyad Safi, Mr. Naim Mohammad and Mr. Irshad Baig.

To my sweet mother and father as well as my siblings, words cannot do the appreciation. May Allah spare your lives on goodness. O my sweetheart and children, Abdullah, Maryam and Ahmad! Thank you for the perseverance while being far away.

Nigerians here in Saudi and back home are very much appreciated for their supports. Mr. Akeem Akinpelu, you are a wonderful brother. The list of those who assisted in the accomplishment of this research in one way or the other cannot be exhausted. Everyone is really appreciated.

TABLE OF CONTENTS

LIST OF TABLES

LIST OF FIGURES

LIST OF ABBREVIATIONS

BET	:	Brunauer Emmett Teller
DI	:	Deionized Water
EDXS	:	Energy Dispersive X-ray Spectroscopy
FGO	:	Few-layered Graphene Oxide
FTIR	:	Fourier Transfer Infra-Red Spectroscopy
GO	:	Graphene Oxide
GPDADMAC	:	Graphene-Poly dially dimethyl ammonium chloride
GPHM	:	Graphene-polymer based 2-hydoxy methyl acrylate
ICP-MS	:	Inductively Coupled Plasm Mass Spectrometer
PDADMAC	:	Poly dially dimethyl ammonium chloride
PHM	:	Polymer based 2-hydoxy methyl acrylate
PZC	:	Point of Zero Charge
RGO	:	Reduced Graphene Oxide
SEM	:	Scanning Electron Microscopy
UV/VIS	:	Ultraviolet–Visible Spectrophotometry
WHO	:	World Health Organization

ABSTRACT

Full Name : Abideen Ojo Salawudeen

Thesis Title : Removal of Phenol and Cadmium from Contaminated Water by Polymeric Modified Graphene Nanomaterials

Major Field : Environmental Sciences

Date of Degree : March, 2019

Phenol and cadmium are among the list of priority pollutants that need to be removed from contaminated water due to their toxic, carcinogenic, mutagenic and persistent nature. This research investigated the capacity of two synthesized graphene-based polymeric nanomaterials in removing phenol and cadmium via adsorption. Graphene functionalized with polymer polydially dimethyl ammonium chloride (GPDADMAC) and polymer based 2-hydroxyethyl methacrylate (GPHM) were utilized for the adsorption of phenol and cadmium ion, respectively. Characterization of both materials was carried out using the Brunauer Emmett Teller (BET), Fourier Transform Infra-Red Spectroscopy (FTIR), Scanning Electron Microscopy (SEM) and Energy Dispersive X-ray Spectroscopy EDXS. The characterization results showed that graphene was successfully functionalized for both adsorbents. Treatment studies using GPDADMAC material revealed that about 80% (1.7 mg/g) of 10 ppm phenol was attained in 10 minutes under the optimum conditions of 4 g/L adsorbent dosage, 298 K temperature, pH of 6 and agitation speed of 150 rpm. On the other hand, GPHM removed more than 60% (0.8 mg/g) of the 0.5 ppm cadmium within 10 min from water using adsorbent dosage of 20 mg, initial solution pH of 7, agitation speed of 200 rpm and temperature of 298 K. Adsorption processes in both cases were best described by the pseudo-second order kinetic model. Moreover, Langmuir and Temkin models fitted

the phenol removal by GPDADMAC while only Temkin fitted the cadmium removal by GPHM. The regeneration study showed that GPHM can be reused after three cycles without much reduction in removal ability. However, GPDADMAC cannot be used for more than one cycle. Using spiked groundwater, the adsorption efficiency dropped from 80% to 49% for phenol and from 60% to 48% for cadmium. This work demonstrated the good potential of GPDADMAC and GPHM for phenol and cadmium removal, respectively.

ملخص الرسالة

الاسم الكامل: عابدين اوجو صلاح الدين

عنوان الرسالة: إزالة أيون الفينول والكادميوم من المياه الملوثة باستخدام مواد نانوية جرافين معدلة بوليمرية

التخصص: العلوم البيئية

تاريخ الدرجة العلمية: رجب 1440

يعتبر الفينول والكادميوم من بين قائمة الملوثات ذات الأولوية التي يجب إزالتها من المياه الملوثة بسبب تأثيراتها السامة والمسرطنة والطفرية. نفذت هذه الدراسة لتقييم قدرة اثنتين من المواد النانوية البوليمرية المركبة و المعتمدة على مادة الجرافين في إزالة الفينول والكادميوم عن طريق الامتزاز(أمتصاص كيميائي). تم استخدام الجرافين المتوافق مع البوليمر ثنائي كلوريد ثنائي دايثيل كلوريد (GPDADMAC) والبوليمر 2-هيدروكسي ايثيل ميثاكريلات -2) hydroxyethyl methacrylate) (GPHM)لإزالة الفينول وايون الكادميوم، على التوالي. تم دراسة الخصائص للمركبين بأستخدام بروناور إيميت تيلر (BET) ، جهاز "فوريه" لتحويل طيف الأشعة تحت الحمراء (FTIR)، المسح المجهري الإلكتروني (SEM) و طيف الأشعة السينية للطاقة المشتتة. وأظهرت نتائج التوصيف أن الجرافين تم تعديله بنجاح في كلتا المواد. وقد اظهرت النتائج ان مادة GPDADMAC أزالت حوالي 80٪ من 10 جزء في المليون (10 ppm) من الفينول في 10 دقائق تحت الظروف المثلى لجرعة ممتززة 6 جم / لتر ودرجة حرارة 298 درجة كلفن وأس هيدروجيني 7 و سرعة مزج 150 دورة في الدقيقة. من ناحية أخرى ، أزال GPHM أكثر من 60٪ من 0.5 جزء من المليون (0,5 ppm) من الكادميوم في غضون 10 دقائق من الماء باستخدام جرعة ممتزة مقدارها 20 ملغ ، وأس هيدروجيني أولي 7 ، وسرعة مزج 200 دورة في الدقيقة ودرجة حرارة 298 درجة كلفن . تم وصف عمليات الامتزاز في كلتا الحالتين بشكل أفضل من خلال النموذج الحركي من الدرجة الثانية. فيما يتعلق بنمذجة isotherm ، قامت نماذج Langmuir و Temkin بتمثيل إزالة الفينول بواسطة GPDADMAC بينما قام Temkin فقط بتمثيل إزالة الكادميوم بواسطة GPHM. باستخدام المياه الجوفية الحقيقية ، انخفضت كفاءة الامتزاز من 80 ٪ إلى 49 ٪ للفينول ومن 60 ٪ إلى 48 ٪ للالكادميوم. لقد أظهر هذا العمل إمكانات جيدة من GPDADMAC و GPHM لإزالة الفينول والكادميوم ، على التوالي.

CHAPTER 1

INTRODUCTION

1.1 Water Pollution by Phenol and Cadmium

Water continues to face various challenges that affect both its quantity and quality. Various factors from both natural and anthropogenic factors such as climate change, urbanization, industrialization and intensive farming activities using pesticides and fertilizers have been identified as being responsible for this water crisis (Larsen et al., 2016). Among the global water issues is the contamination by organic and inorganic compounds, which are mostly toxic and carcinogenic to organisms and human beings (Sousa et al., 2018; Abbas et al., 2016; Liu et al., 2008). Coupled with the fact that most of these contaminants are non-biodegradable, they are persistent in the natural environment as well as bioaccumulate and biomagnify in the food chain and food web. Notable among the toxic organic and inorganic pollutants are phenol and cadmium.

Phenol is among the priority water pollutants identified by the United States Environmental Protection Agency (USEPA) that calls for great attention due to its toxic nature, persistence in the environment, biomagnification in organisms and damaging health effects in human (Pradeep et al., 2015). Due to health danger of phenol, any drinking water is expected not to exceed the maximum allowable level of 0.002 mg/L according World Health Organization (Srivastava et al., 1997). The ingestion of water contaminated with phenol over a long time causes destruction of body protein and tissues, dysfunction of the central

nervous system and damages to the gastrointestinal tract. Phenol is released into the environment through various sources, including industries that use it as raw materials such as dyes, textiles, pesticides, insecticides, disinfectants, antiseptics and explosive industries, and other industries that generate it as waste product such as leather, steel, olive oil manufacturing and phenol production industries (Villegas et al., 2016).

Similarly, cadmium is among the harmful trace metals that can be found in water, food and environment (Friberg, 2017). Acute or chronic exposure leads to systemic effect such as kidney, liver and pancreas damage, respiratory effect, carcinogenic and genetic effect (Chabicovsky et al., 2004; Faroon et al., 2012). Due to its detrimental effects when consumed, the World Health Organization stipulates 0.003 mg/l as the maximum allowable limit of cadmium in drinking water (Izah et al., 2016). Its sources include coal burning, iron and steel processing, production and use of phosphate fertilizer manufacture and so on. It is one of the priority harmful metals which is ranked 7^{th} among the top 20 contaminants according to USEPA (Rehman et al., 2017; Carolin et al., 2017).

A random survey of literatures revealed the contamination of some groundwater in Saudi Arabia with cadmium. The wadi Fatimah groundwater (Sharaf and Subyani, 2011) and some ground waters in the south Al-Madinah Al-Munawarah (El Maghraby et al., 2013)were found to contain a higher cadmium concentration beyond safe drinking limit. Phenol is more common in some wastewater from industries in Saudi Arabia such as the olive mill (Aly et al., 2014)

As water regulations and standards become more stringent, the need for phenol and cadmium removal from contaminated water becomes more crucial. Thus, it is imperative

to remove phenol and cadmium ions in contaminated wastewaters prior to their discharge or before being used for domestic purposes.

Over years, the potential of several decontamination techniques has been investigated for the treatment of water contaminated with phenols and cadmium ions (Busca et al., 2008; Villegas et al., 2016; Carolin et al., 2017). Regarding the removal of phenol and cadmium from contaminated water, common technologies used include photocatalytic degradation (Shet and Vidya, 2016), ozonation (Biglari et al., 2017), extraction method (Liu J.et al., 2013), biological method (Liu C.et al., 2016), membrane-based separation (Cui et al., 2016), electrochemical advanced oxidation method (Mousset et al., 2016), ion exchange (Víctor et al., 2016) as well as coagulation, ion exchange and electrodialysis (Mohammadi et al., 2014).

However, various disadvantages have been associated with most of these methods. For example, high chemical use and post-treatment sludge production are among the drawbacks of coagulation (Fajardo et al., 2015). High cost and membrane fouling are associated with membrane filtration (Villegas et al., 2016). Clogging, prolonged treatment time, high electrical power demand and limited metal ion removal are some of the drawbacks of electrodialysis, photocatalysis, electrochemical processes and ion exchange, respectively (Mohammadi et al., 2014).

Consequently, adsorption is considered among the best available technology for the remediation of water containing phenol and cadmium due to its inexpensiveness and effectiveness (De Gisi et al., 2016). The technique produces no toxic wastes. However, its performance is highly constrained by material design and properties (Saleh, Tuzen and Sarı

2017). For instance, the fairly long time it usually takes to adsorb phenols and cadmium with most adsorbents is a challenge. Moreover, there are usually other challenges of low adsorption capacity and difficult recovery process with most adsorbents.

The application of nanotechnology in water treatment has helped a great deal in developing highly efficient procedures to produce nanoadsorbents of exceptional attributes (Wang et al., 2014; Asmaly et al., 2015; Wang and Chen, 2015; Asmaly et al., 2016; Burakov et al., 2018; Thines et al., 2017). Carbon-based adsorbents, including activated carbon and nanotubes, have been always at the center of attraction. However, their activity is limited to the surface area.

Recently, the use of graphene as a novel adsorbent for wastewater remediation is gaining popularity (Peng et al., 2017; Wu et al., 2015; Liu et al., 2016; Gupta et al., 2013; Saleh et al., 2017). This is attributed to its unique characteristics, among which are high specific surface area as well as uncomplicated synthesis from graphite by following cheap method involving chemical oxidation, exfoliation and reduction. The use of graphene in adsorption process has spanned a wide number of contaminants, which includes different types of dyes (Ji et al., 2013), metal ions (Chowdhury and Balasubramanian, 2014) and organic pollutants (Zeng et al., 2013).

However, the tendency of graphene and its derivatives to aggregate to reform graphite and their weak affinity for binding anionic pollutants are disadvantageous to their applications (Park and Yan, 2012). Nevertheless, these disadvantages are surpassed by employing various forms of functionalization with diverse molecules. This surface functionalization makes graphene and its relatives more sensitive, selective and detective. Polymer

functionalization confers the characteristics of stable dispersion and optimized microstructure on graphene (Fang et al., 2009). Due to the availability of many materials that can be used for surface functionalization, exploration of the potentials of the different materials in treating contaminated water is gaining more attention (Luo et al., 2013). A large number of reports exist on the successful synthesis and use of several functionalized graphene and its derivatives as adsorbents for water treatment (Upadhyay, 2014).

Materials used for functionalization of graphene include organic polymers and nanosized metal oxide (Bolto and Gregory, 2007). These materials can be grafted on the surface without any requirement of cross linkers, which usually reduce the binding sites for pollutants.

1.2 Characteristics of Graphene

Graphene is an allotrope of carbon discovered in 2004, making it the most recent of all carbon allotropes (Peng et al., 2017). Its structure is a single layer of carbon similar to graphite and also has a partially infinite size similar to polycyclic aromatic hydrocarbon. Thus, graphene (Fig 2.1) has a 2D honeycomb network of hybridized sp2 carbon atoms which are densely organized to form single flat structure (Chowdhury and Balasubramanian, 2014; Punetha et al., 2017).

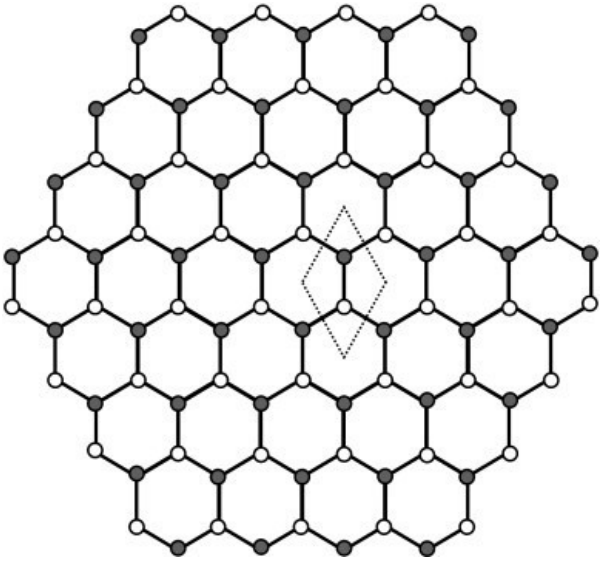

Figure 1.1: Lattice structure of graphene (Chowdhury and Balasubramanian, 2014)

Graphene has several unique properties which give it wide applications (Table 1.1) which include a comparatively large surface-to-volume ratio. In addition, its special ductility and brittleness make it the ever known thinnest and strongest material (Xin et al., 2015). As a result of all these unique properties of graphene, it finds a good application in different areas of research such as in biomedical, electronics and production of structural composites, electrodes, polymers and so on (Perreault et al., 2015).

Recently, graphene is seen as one of the novel adsorbents for wastewater remediation is gaining more popularity (Wang et al., 2014; Peng et al., 2017). This is attributed to its unique characteristics, among which are high specific surface area and easy synthesis from graphite by following an uncomplicated and cheap method involving chemical oxidation, exfoliation and reduction. It has been applied for the adsorption of dyes (Hosseinabadi-Farahani et al., 2015), metal ions (Yari et al., 2015) and organic pollutants (Yu et al., 2015).

Most applications of graphene as adsorbent for the removal of various pollutants in aqueous media involves using it in various forms, such as graphene nanosheets, graphene oxide (GO), reduced graphene oxide (RGO), and few-layered graphene oxide (FGO) as well as nanocomposites. This is made possible by their modifiable chemical properties and possession of large pi-electrons as well as huge surface area.

1.2.1 Preparation of Graphene

There are several ways by which the synthesis of graphene can be carried out. Generally, the various synthesis methods can either be a top-down or a bottom-up approach (Zhu et al., 2010; Edwards and Karl, 2013). In the top-down category, various processes are used to subject stacked layers of graphite to forces high enough to cleave the weak van der Waal bonds between its graphene layers. It is the earliest method by which graphene sheets were produced by the mechanical cleavage of graphite. It involves processes such as mechanical cleavage, electrochemical exfoliation, exfoliation of graphite intercalation compounds (solvent-assisted and thermal exfoliation.), solvent-based exfoliation, exfoliation of graphite oxide, arc discharge and unzipping carbon nanotubes. The stumbling blocks with these methods include damaging and re-agglomeration of the synthesized graphene sheets. It is also characterized with low graphene output following numerous steps. The use of graphite as a precursor material in this approach necessitates the tedious mining and processing before it can serve as a starting material.

Meanwhile, the different methods of bottom-up approach entail the use of alternative carbon-containing sources as precursors for graphene. Generally, the approach requires subjecting precursor materials to high temperature in order to graphitize. It has the advantages of being able to produce graphene films with large area following usually

simple steps. However, it leads to more morphological defects in the produced sheets than the top-bottom approach. The bottom-up methods include epitaxial growth on silicon carbide and chemical vapor deposition such as growth on metals and substrate free. Table 1.2 summarizes the various types of the preparation methods (Mittal et al., 2015).

1.2.2 Functionalization of Graphene

Functionalization of graphene involves bonding different organic functional groups to its surface through chemical processes. The functional groups, which are provided by organic solvents in the presence of a stabilizer or an additive, are covalently or noncovalently bonded to graphene through various chemical reactions such as oxidation and deposition as well as electrochemical, sol-gel, microemulsion, and hydrothermal techniques (Georgakilas et al., 2012). The functionalization processes involving pure chemical reactions such as oxidation and deposition have the advantages of achieving desired functional groups in a simple way. It is also possible to produce multi-functional graphene through the integration of several functional groups.

Covalent functionalization of graphene is carried out by making a mixture of graphene in organic solvents which are usually nonpolar. The process of covalent functionalization has been identified to follow two mechanisms, either covalent bonds are created between free radicals and the carbon-carbon double bonds of graphene or the covalent bonds connect the organic functional groups with the oxygen groups of graphene oxide (Kuila et al., 2012). However, due to the hydrophobic nature of graphene which makes them insoluble in polar solvents, noncovalent functionalization is a very crucial process for obtaining a mixture of graphene in common polar organic solvents. In contrast to covalent functionalization, noncovalent functionalization attaches the functional groups without any

disturbance to the electronic network of graphene viz the extended π-conjugation on the graphene surface. It also prevents the agglomeration of graphene layers in polar organic solvents (Cai and Song, 2010).

Table 1.1: Graphene Properties

Physical properties (Chowdhury and Balasubramanian, 2014)	**Chemical properties** (Sheka, 2014)
Carbon-carbon bond length = 0.142 nm	sp2 Configuration of the atom valence electrons yielding a perfect flat 2D structure of condensed benzenoid units
Theoretical BET-specific surface area = 2630 $m^2\ g^{-1}$	Very strong carbon-carbon valence bonds
Density = 0.77 mg m^{-2}	
Carrier density = 10^{12} cm^{-2}	
Resistivity = 10− 6 Ω cm	
Fracture strength = 125 GPa	
Young's modulus = 1100 GPa	
Optical transparency = 97.7%	
Thermal conductivity = 5000 W $m^{-1}\ K^{-1}$	
Electron mobility = 200,000 $cm^2\ V^{-1}\ s^{-1}$	

Table 1.2: Preparation methods for graphene (Mittal et al., 2015)

Bottom-Up Techniques (growth on surfaces)		**Top-Down Techniques**	
Epitaxial growth (Thermal Decomposition)	**Chemical vapor deposition (CVP)**	**Exfoliation method**	**Other methods**
1. Growth on silicon carbide	1. Growth on metals	1. Electrochemical exfoliation	1. Arc discharge
2. Growth on other substrates	2. Substrate free	2. Mechanical exfoliation	2. Unzipping carbon nanotubes
	3.Plasma-enhanced CVP	3. Exfoliation of graphite intercalation compounds	3. Chemical extraction from graphite without exfoliation
	4.Thermal CVP	4.Solvent-based exfoliation	
		5. Exfoliation of graphite oxide	

CHAPTER 2

LITERATURE REVIEW

The continuous expansion of human activities connected to agriculture, domestic and industries has led to an increased generation of harmful pollutants which are not uncommon in the surrounding water bodies (Fernandez et al., 2018; Bazrafshan et al., 2016). Most of these water pollutants are of great concern because of their persistent nature as well as bioaccumulation. They constitute danger to the survival of both aquatic and terrestrial organisms as well as human health due to their carcinogenic and mutagenic attributes. Cadmium ions and phenols are among the inorganic and organic pollutants of serious concern. With stricter water regulations on the level of contaminants, the level of researches in water treatment has stepped up over recent years to develop new water treatment technologies as well as improve the existing techniques.

Generally, adsorption is seen as one of most assuring technique for the treatment of contaminated water (Chowdhury and Balasubramanian, 2014). Its increasing wide acceptance as a removal technique has been attributed to its inherent advantages of low capital cost, flexibility and simplicity in design and operation, production of no sludge and toxic by-products, regeneration and reuse ability as well as outstanding removal of organic and inorganic contaminants (Albadarin et al., 2017; Mohanty, Das and Biswas 2005; Tripathi and Ranjan, 2015).

Adsorption is an interfacial phenomenon that involves the attachment of a substance (called the adsorbate) onto the surface of another substance (called the adsorbent) (Mohammadi et

al., 2014). The process of adsorption depends on the states of matter of adsorbate and adsorbent. The process is said to occur at liquid-liquid interface if the adsorbate medium and the adsorbent are both liquid. On the other hand, the process can also occur at gas-liquid interface if the adsorbate medium is gas and the adsorbent is liquid. Whenever the adsorbate medium and the adsorbent are gas and solid, adsorption process occurs at gas-solid interface. Of the different types of the interfacial adsorption processes, liquid-solid interface is of paramount significance in industries and everyday life (Rouquerol et al., 2013).

Some forces have been identified to influence the uptake of the adsorbate by the adsorbent. Adsorption processes in which weak forces of attractions, such as van der Waals, are predominant in bringing about the physical attachment of the adsorbate to the adsorbent surface are said to be physisorption. This kind of adsorption processes is characterized by reversibility of the process because of the presence of the weak forces. Meanwhile, processes involving chemical bonding between the adsorbate and the adsorbent are called chemisorption. Their forces are stronger than that of physisorption and as such it is not easy to break the adsorbate from the adsorbent surface. However, the two processes of physisorption and chemisorption occur simultaneously or alternatively in most systems (Faust and Aly, 2013).

Various materials are used for the adsorption of the existing and growing number of pollutants (Malik et al., 2017). Adsorption using activated carbon is highly preferred because of its of high porosity and large surface area. However, its limitation in terms of relatively high cost has hampered its widespread use (Mohammadi et al., 2014). In a search for a less costly alternative, researchers have continued to investigate the potentials of

many ligno-cellulosic materials as replacement for activated carbon. These materials have come from various sources including waste and by-products from industrial, agricultural and domestic activities such as fly ash (Olabemiwo et al., 2017), sewage sludge (Liadi et al., 2018), olive stone (Bohli et al., 2015), natural materials such as clays (Thue et al., 2018) and zeolites (Pham, Lee and Kim, 2016). Although these materials are of relative low cost, majority of them have low performances in the adsorption of contaminants (Sherlala et al., 2018) including phenol and cadmium.

In recent years, advancement in material science and engineering as well as its application in water treatment technology has led to the synthesis of novel adsorbents for contaminant removal from aqueous medium. Different nanomaterials with carbon as building block such as carbon nanotubes (CNTs) as well as chitosan, complexing membrane and modified iron oxide have been reported as adsorbents for both inorganic and organic contaminants (Ehrampoush et al., 2015; Zare et al., 2015; Nguyen et al., 2016). Their increasing popularity is linked to their special and novel morphological and structural characteristics. Undoubtedly, there has been much progress on their application in adsorption over the recent decades (Abbas et al., 2016). However, the limitation imposed by their expensive fabrication process, especially the CNTs, has constrained their feasible commercial applications (Sherlala et al., 2018). Therefore, it is expedient to investigate the potential of new promising adsorbents.

Most recently, graphene-based adsorbents are among the most new materials that have been explored for their treatment of contaminated water as a result of their exceptional properties which include high specific surface area and easy synthesis from graphite by

following an uncomplicated and cheap method involving chemical oxidation, exfoliation and reduction.

2.1 Adsorption of Cadmium and Phenol by Graphene

The adsorption of phenol and cadmium ions by graphene and its family have been studied by several authors which indicate the good potential adsorption capacity of graphene for phenol and cadmium (Wang et al., 2014; Peng et al., 2017; Yu et al., 2015).

Using a modified Hummer's protocol, Mukherjee et al. (2017) prepared graphene oxide for phenol adsorption under the influence of ultrasonic irradiation. The adjustments of various parameters resulted in the adsorption capacity reaching a maximum of 10.23 mg g^{-1} after 120 minutes when the initial concentration of phenol was 20mgL^{-1}, adsorbent dosage of 1gL^{-1}, temperature of 303 K, pH of 6.3 and stirring rate of 140rpm.

The comparison of the adsorption efficiencies of 2D graphene nanoplates and other carbon nanomaterials free of metals for phenol was investigated by Indrawirawan et al. (2015). The best adsorption was obtained using the 2D graphene nanoplates and 3D hexagonally-ordered mesoporous carbon among the materials. About 40% phenol was removed in 500mL of 20ppm solutions at 0.2 g/L adsorbent dosage, pH of 6.5-7, temperature of 25 °C within 180 minutes.

Graphene oxide can be produced from different materials. Zhang et al. (2017) investigated the difference in Cd^{2+} adsorption capacities of graphene oxide synthesized from two different materials, flaky graphite and amorphous graphite. The experimental conditions of 10 mg/L adsorbent dosage, 60 mg/L initial cadmium concentration, agitation speed of 150 rpm, contact time of 12 h and temperature of 25 °C were applied on the adsorption by

the two materials. The results showed that amorphous graphite-based graphene oxide has a larger adsorption capacity of 1792.6 as against 260.9 mg g^{-1} of flaky graphite-based graphene oxide.

Wang and Chen, (2015) carried out an investigation on the difference in the adsorption and coadsorption of Cd^{2+} with some organic compound using GO and two RGO materials produced by chemical reduction and annealing. The strongest affinity for Cd^{2+} was obtained with graphene oxide. Also, the adsorbed Cd^{2+} on the GO and chemically produced RGO enhanced the coadsorption of naphthalene and 1-naphthol.

The importance of varying experimental parameters in order to arrive at optimum conditions and obtain good adsorption by graphene is crucial. Li et al. (2012) studied the influence of some experimental parameters on the adsorption of phenol by a prepared graphene. The adsorption capacity got to a maximum of 28.26 mg/g with pH of 6.3, temperature of 285 K and the initial phenol concentration of 50 mg/L.

The types of functional groups possessed by graphene plays a very crucial role in determining its adsorption capacity. Bian et al. (2015) studied the influence of the oxo-functional group present in graphene oxide on the adsorption of Cd^{2+}. They obtained 23.9 mg/g as the highest adsorption capacity when adsorbent dosage, shaking speed, contact time and pH range were 1g/L, 200 rpm, 4 h and 6.0–7.0 respectively.

Application of graphene in the treatment of real wastewater was studied by Wang et al. (2015). They investigated the removal efficiency of a 3D graphene aerogels-mesoporous silica frameworks for various phenols in domestic sewage and industrial wastewater. The adsorption results showed a 68.6% removal efficiency for phenol at experimental

conditions of contact time, temperature and adsorbent dosage of 2 h, 25 ± 2 °C and 0.002 g/ml, respectively. The adsorption capacity reached maximum of 90 mg/ g within 24 h of contact.

Zhao et al. (2011) investigated sorption efficiency of graphene oxide nanosheets composed of few layers for $Cd^{2+}$and Co^{2+}in a single aqueous system. The highest adsorption capacity for cadmium ion was about 106.3 mg/g as compared to 68.2 mg/g of Co (II) at pH of 6.0 ± 0.1 and temperature of 303 K.

Pollutants coexist in aqueous solution. Sitko et al. (2013) studied the adsorption of Cd^{2+}, Cu^{2+}, Zn^{2+}, and Pb^{2+} by graphene oxide nanosheets synthesized from oxidation of graphite by potassium dichromate from a single and multi-aqueous system. The capacity of the adsorbent was greater to remove Cd^{2+} than other metals except Pb^{2+}in the single aqueous system and it was 530 mg g^{-1}. Also, Cd^{2+} adsorption in the multi-aqueous solutions was higher than other metal except Zn^{2+}.

Similarly, Tan et al. (2015) reported their results on the adsorption of $Cu^{2+,}$ Cd^{2+} and Ni^{2+} by graphene oxide membranes from a single aqueous solution. Among the metals, the material has the highest adsorption capacity 83.8 mg g^{-1} for Cd^{2+} when the temperature, shaking speed, initial adsorbate concentration, adsorbent dosage and pH were 303 K, 200 rpm, 20 mg/L, 0.2 g/l and 5.8, respectively.

2.2 Functionalized Graphene for Phenol and Cadmium Removal

The fabrication of a 3D sulfonated reduced graphene oxide and the investigation of its adsorption capacity for cadmium (Cd^{2+}) in a single solute solution was reported by Wu et al. (2015). Around 93% of Cd^{2+} was adsorbed within 20 minutes when the adsorbent dosage

and initial Cd^{2+}concentration were 0.1 g/L and 2 mg/L respectively. At pH of 6.0 and temperature of 298 K, the maximum adsorption capacity was 234.8 mg/g.

In the work of Li et al. (2016), plasma technique was applied to prepare nanoscale zero-valent iron particles on reduced graphene oxides. They studied the capacity of the synthesized material to adsorb Cd^{2+} from single metal solution. The maximum adsorption capacity of 425.72 mg g^{-1} was obtained when the adsorbent dosage was 0.1 g L^{-1}, initial concentration of Cd^{2+} was 150.0 mg L^{-1} at temperature of 293 K and pH of 5.0.

Similarly, Hu et al. (2015) prepared a novel adsorbent from graphene oxide and polypyrrole using the dielectric barrier discharge plasma technique and studied the removal efficiency of the composite for phenol and aniline. The adsorption capacity reached maximum of 2.14 mmol·$g^{-1}$when phenol concentration, adsorbent dosage, pH and temperature were 20.0 mg L^{-1}, 0.2 g L^{-1}, 6.0 and 298 K, respectively.

Gong et al. (2016) carried out study on selective adsorption capacity of graphene oxide integrated with poly (N-isopropylacrylamide) for different phenols. From their results, maximum adsorption capacity for phenol was 12.7425 mg/g equivalent to about 4 times that of non-grafted graphene oxide when the phenol concentration was 25 mg/L, temperature of 25 ± 0.1 °C, pH of 7.0 ± 0.1, shaking speed of about 140 rpm and adsorbent dosage of 0.1g/L.

Hu et al. (2014) prepared sulfanilic acid-grafted magnetic graphene oxide sheets (MGOs/SA) and examined its adsorption capacity in a binary solute solution of cadmium and aniline. Their results showed that MGOs/SA was effective in removing both pollutants. However, the adsorption was strongly influenced by solution pH. The presence of aniline

in the solution reduced the adsorption of cadmium above the pH of 5.4 while it enhanced cadmium adsorption at a pH below 5.4. In the same vein, adsorption of aniline was increased when the pH was above 7.8 while it reduced at pH values lower than 7.8.

2.3 Problem Statement

Improvement of the removal ability of graphene for phenol and cadmium is of great importance for the purification of water. This improvement entails modification of graphene in order to get rid of its disadvantageous characteristics of agglomeration and weak affinity. Polymer functionalization of graphene improves its dispersion stability which prevents its aggregation into graphite that reduces adsorption capacity. In addition, functionalization helps in improving the ease of processing and also enhances binding of pollutants of both organic and inorganic nature on the surface of graphene. Materials used for functionalization of graphene include organic polymers and nanosized metal oxides.

Therefore, this study investigated the removal efficiency of a graphene nanomaterial modified with two different polymeric materials for the adsorption of phenol and cadmium separately from spiked deionized water and spiked groundwater samples. Graphene grafted with polymer polydially dimethyl ammonium chloride (GPDADMAC) and polymer based 2-hydroxyethyl methacrylate (GPHM) were investigated for their adsorption of phenol and cadmium, respectively. The influence of various parameters including pH, agitation speed, temperature, contact time, initial concentration and adsorbent dosage on the adsorption process was evaluated. Adsorption experimental data were tested on different kinetic models and isotherm models. Lastly, the thermodynamic parameters such as change in entropy, enthalpy and free energy change were also obtained for the processes.

CHAPTER 3

RESEARCH OBJECTIVES

The primary aim of this study was to evaluate the adsorption efficiency of two polymeric modified graphene nanomaterials GPDADMAC and GPHM to remove phenol and cadmium ions from a single solute aqueous system. The specific objectives are to:

1. Characterize the synthesized polymeric modified graphene nanoparticles before the adsorption experiment.
2. Assess the removal of phenol by GPDADMAC and cadmium ions by GPHM from synthetic water.
3. Optimize treatment conditions such as temperature, adsorbent dosage, initial adsorbate concentration, agitation speed, pH as well as contact time.
4. Develop isotherms and evaluate adsorption kinetics under the optimum treatment conditions and compare with the adsorption with a standard activated carbon removal capacity.
5. Investigate the regeneration ability of the adsorbents
6. Use the optimum treatment conditions to assess phenol and cadmium ions removal capacity of the synthesized GPDADMAC and GPHM in real groundwater.

CHAPTER 4

MATERIALS AND METHODS

4.1 Chemical Reagents

Analytical grade of all reagents were utilized for the experiments. One gram of phenol (Sigma-Aldrich, >99%) was dissolved in 1L of ultra-pure deionized (DI) water generated by Milli-Q Ultrapure water system (Millipore) to obtain a stock solution of 1000 mg/L of phenol. Thereafter, working solutions of desired concentrations were prepared in clean conical flasks by diluting appropriate volume of the stock solution with appropriate volume of DI water.

For the preparation of stock solution of cadmium, cadmium nitrate supplied by ULTRA Scientific (USA) (>99% Sigma-Aldrich) was used by adding 10 ml of 1000 ppm standard to a 190 ml deionized water in a 200 ml conical flask. Subsequently, working solutions of 2 ppm, 4 ppm, 6 ppm, 8ppm and 10 ppm were prepared by making the appropriate dilution. For experiments requiring pH adjustment, 0.1 M HNO_3 (Merck, Suprapure) or 0.1 M NaOH (Merck, Suprapure) solution was used and the pH was ascertained by benchtop pH meter (A0057419, Hanna).

Other chemical reagents used were potassium persulfate ($K_2S_2O_8$) (Sigma-Aldrich), sulfuric acid (H_2SO_4) (Sigma-Aldrich), $KMnO_4$ (Sigma-Aldrich), HCl (Sigma-Aldrich), 2-hydroxyethyl methacrylate (99.5% percent weight, Sigma-Aldrich), ethylene glycol dimethacrylate (EGDMA) (0.5% percent weight, Merck company), ammonium peroxo disulfate (Sigma-Aldrich), sodium disulfite (Sigma-Aldrich), ethanol (Sigma-Aldrich),

acetone (Sigma-Aldrich), dimethyl amine (Sigma-Aldrich), allyl chloride (Sigma-Aldrich), tert-Butyl hydroperoxide (tBuOOH) (Sigma-Aldrich).

4.2 Synthesis of Adsorbent Materials

4.2.1 Synthesis of graphene oxide (GO)

Graphite powder was used as base material for the preparation of graphene oxide according to the Hummer's method. 1.8 g of potassium persulfate ($K_2S_2O_8$) and 3 g of natural graphite powder were added into 100 mL sulfuric acid in an ice-water bath, under stirring. Then the mixture was heated to around 90 ℃ in an oil bath. Then, the system was allowed to cool. After that, 9 g of $KMnO_4$ were added into the flask slowly. Then, the system was heated at around 40 ℃ under stirring. After that carefully, water and hydrogen peroxide 30% were added (30%) till the brownish color was observed. The filtration and washing of the mixture were done with dilute 2 M HCl aqueous to remove metal ions. The final wash was done with deionized water to ensure the sample has a neutral pH. The obtained sample was collected and dried in vacuum freezing drying oven for 2 days.

4.2.2 Synthesis of polydially dimethyl ammonium chloride (PDADMAC)-graphene oxide (GPDADMAC)

First, the monomer was created by reacting equivalent amounts of allyl chloride and dimethylamine. The polymer was then produced by radical polymerization of diallyldimethylammonium chloride in presence of graphene of which the functional groups were utilized to host the monomer. Then, organic peroxide was introduced to the system as a catalyst for the radical polymerization. When polymerizing diallyldimethylammonium chloride, one side of the polymer chain is chemically bonded on graphene and the chain is grafted, as shown in Fig. 4.1.

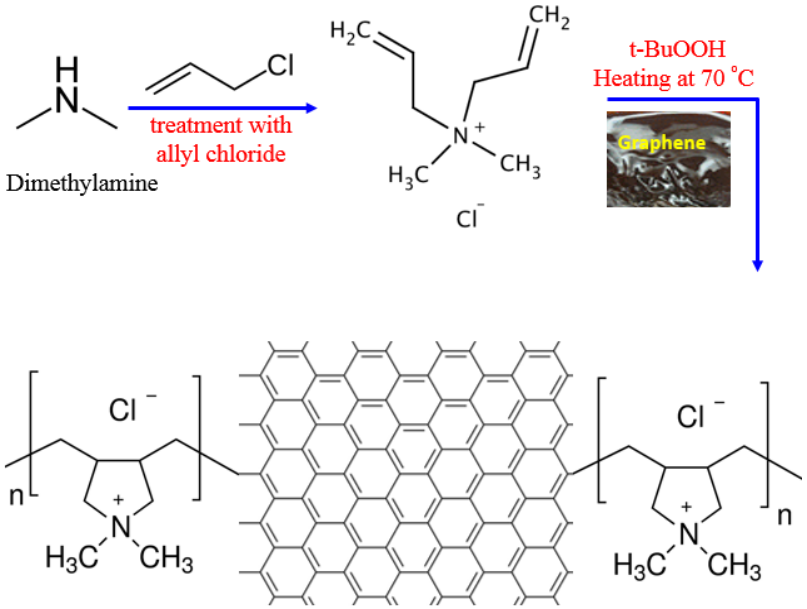

Figure 4.1: Illustration of the process of synthesizing polydially dimethyl ammonium chloride modified graphene (PDADMAC).

4.2.3 Synthesis graphene grafted with polymer based 2-hydroxyethyl methacrylate (GPHM)

In the fabrication of poly (2-hydroxyethyl methacrylate), 99.5% percent weight of 2-hydroxyethyl methacrylate as a monomer, 0.5% percent weight ethylene glycol dimethacrylate (EGDMA) as cross-link agent (from Merck company), ammonium peroxo disulfate and sodium disulfite as initiators were used. These components were added into dispersed (by sonication) graphene nanosheets at room temperature with 30 rpm stirring for 16 h. Further polymerization of the mixture was carried out at 70 °C for 16 h with 400 rpm stirring.

The resulting polymer was repeatedly rinsed with ethanol. The polymer in the mixture was hydrolyzed by 130 ml of 0.4 M NaOH at room temperature for 2 days and at 75 °C for around 16 h under stirring. The obtained GPHM was washed acetone, and several times

with deionized water and kept dry. The illustration of the GPHM functionalization process is displayed in Fig. 4.2 below.

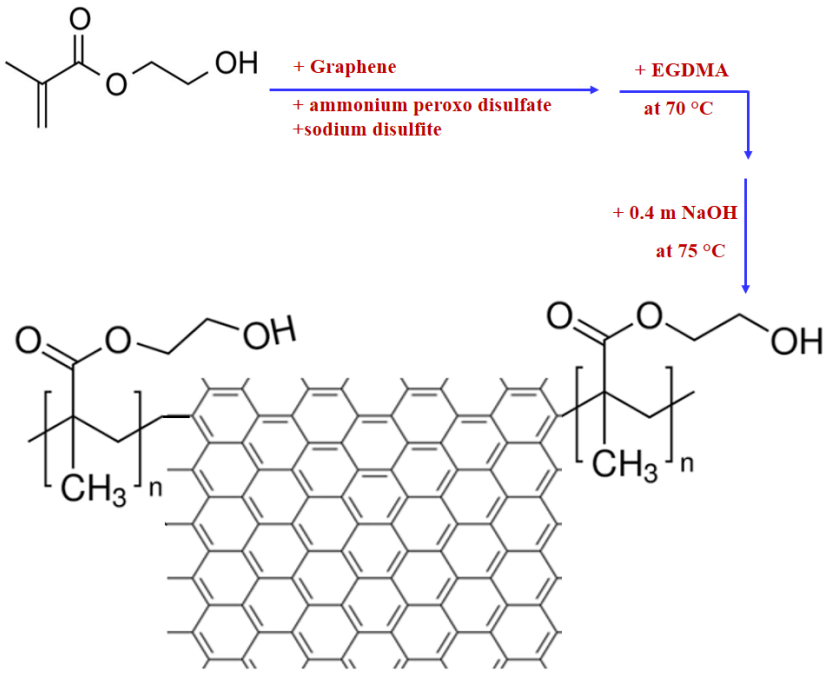

Figure 4.2: Illustration of the synthesis of graphene grafted with poly 2-hydroxyethyl methacrylate (GPHM).

4.3 Instruments for Characterization

4.3.1 Morphological Structure of Adsorbent Surface

The surface shapes and the pore structure of GPDADMAC and GPHM were assessed by Scanning Electron Microscope (SEM) coupled with Energy Dispersive X-ray Spectrometer (EDX) (TESCAN LYRA3). Images at different magnifications were obtained. Meanwhile, the determination of the surface elemental compositions of both GPDADMAC and GPHM was carried out by EDX.

4.3.2 Surface Area (Brunauer–Emmett–Teller (BET)), Pore Distribution and Characteristics

The determination of the surface area and porous distribution were carried out by nitrogen physisorption at -196ºC using Micrometric ASAP 2000 system.

4.3.3 Functional Groups Determination

Functional groups detection for GO, GPDADMAC and GPHM was done using FTIR spectrum produced by FTIR Spectrometer (Nicolet 5700 FT-IR Thermo Electron Corporation) over the wave number range from 4000 to 400 cm^{-1}. The samples for FTIR were pelletized using pressed disks to grind and mix samples with KBr in an agar mortar.

4.4 Point of Zero Charge (PZC) Determination

The PZC for GPDADMAC and GPHM were determined by the following procedure by Thirumavalavan et al., (2009). An Erlenmeyer flask was filled with 100 ml of DI water and capped with cotton wool. This was heated until boiling for about 30 min to expel all carbon dioxide and dissolved ions in the water. Immediately after cooling, the flask was capped with rubber stopper to prevent carbon dioxide from entering. 10 ml of this carbon dioxide free DI water was added to about 30 mg of the adsorbent, sealed and shaken for 48 hrs at room temperature of 25 ºC. The final pH of the solution was measured and taken as the PZC of the adsorbent.

4.5 Characterization of Groundwater Sample

The efficiency of GPDADMAC and GPHM were evaluated in a groundwater sample obtained from the waterwell 1 near Building 26 in KFUPM campus. Prior to the treatment of the spiked groundwater water, the anions and cations were determined using Metrohm AG - 850 Professional Ion Chromatography. The eluent for the anion was sodium

carbonate at 0.700 mL/min flow rate while the eluent for the cation was Nitric Acid at 0.800 ml/min flow rate.

4.6 Treatment studies

Batch adsorption experiments were carried out to evaluate the removal efficiency of GPDADMAC for phenol and GPHM for cadmium. For each experiment, 50 ml of aqueous solution of either phenol or cadmium in 250ml Erlenmeyer flasks was used to study the effect of initial solution pH, agitation speed, temperature, adsorbent dosage, initial concentration of phenol, and contact time. A 0.45 µl filter was used to separate the filtrate after every experimental run. For phenol measurement, a single output from the UV/VIS spectrophotometer (at wavelength of 271nm) is a mean value generated automatically from three measurement runs. To ensure repeatability, the mean of two replicates was used in the computation of percentage removal as well as adsorption capacity as per the following equations (Olabemiwo et al., 2017):

$$\%\ adsorbate\ removal\ = \frac{(C_i\ -\ C_f)}{C_i}\ \times\ 100$$

$$Adsorption\ capacity\ = (C_i\ -\ C_f)\ \times \frac{V}{m}$$

C_i (mg/L) and C_f (mg/L) stand for initial and final concentrations of phenol or cadmium whereas V (mL) and m (mg) are the volume of aqueous solution containing phenol or cadmium and mass of adsorbent of GPDADMAC or GPHM, respectively. Also, the concentrations of the blanks were measured before and after every experiment.

4.6.1 Adsorption isotherms

In order to design a suitable industrial adsorption system, it is crucial to know the distribution of adsorbate molecules between the adsorbent and the adsorbate solution as well as the interactions between both (Ayawei, Augustus and Donbebe, 2017). Towards this end, several adsorption isotherm models are applied on adsorption data to obtain the best-fit models. Application of isotherm models is based on the general assumptions concerning interaction of adsorbate with adsorbent, number and nature of adsorbent layers involved in adsorbing the adsorbate. Langmuir, Freundlich and Temkin are some of the empirical isotherm models mostly applied to single solute systems carried out in batch mode.

Langmuir isotherm models are used to show the relationship between the amount of adsorbate attached to homogenous surface of a single layer of an adsorbent and its equilibrium concentration in aqueous solution. It assumes strong attachment of the adsorbate molecules to a limited number of sites, of homogenous sorption energies, found on only one layer of the adsorbent. Its linear mathematical expression is given as:

$$\frac{C_e}{q_e} = \frac{1}{K_L . q_m} + \frac{q_e}{q_m}$$

where K_L (L/mg) is the constant for sites of adsorption affinity on homogenous monolayer surface, q_m (mg/g) represents the maximum monolayer adsorption capacity, q_e (mg/g) is the amount of adsorbate adsorbed, C_e (mg/L) is the equilibrium concentration of adsorbate in solution.

The values of q_m and K_L are obtained from the slope and intercept of a plot of C_e/q_e against C_e.

Another important factor computed from Langmuir model is the separation factor given by:

$$R_L = \frac{1}{(1 + K_L . C_o)}$$

C_O (mg/L) denotes the initial adsorbate concentration. R_L is a dimensionless equilibrium parameter that indicates how favorable an adsorption process occurs. The value of R_L is interpreted as follows:

Value of 1 is an indication of a linear adsorption, value greater than 1 indicates an unfavorable adsorption process, between 0 and 1 means favorable adsorption process while equal to 0 indicates irreversible adsorption process (Wang and Chen, 2015).

Freundlich isotherm model is another empirical model that gives a better description of a non-ideal and reversible adsorption process over a large span but of lower concentrations. It assumes that the adsorbate molecules are adsorbed on surfaces possessing different sorption energies found on several layers of the adsorbent.

Its linear mathematical form is:

$$ln\ q_e = ln\ K_F + \frac{1}{n}\ ln\ C_e$$

K_F (mg/g) represents a constant that indicates adsorption capacity. A high value of K_F is an indication of high adsorption capacity.

The heterogeneity parameter, n, gives the description of adsorption intensity. A value of n equal to 1 indicates a linear adsorption where all adsorption sites have the same sorption

energies. When *n* is greater than 1, it implies a normal and favorable adsorption process and the higher its value, the stronger is the adsorption.

C_e (mg/L) and q_e (mg/g) are the adsorbate concentration in solution and amount of adsorbed adsorbate on the adsorbent, respectively.

The values of n and K_f are obtained from the slope and intercept of the graph of $ln\ q_e$ versus ln C_e.

Temkin isotherm model works on the assumption that the relationship between the adsorbate and the adsorbent causes a linear decrease in sorption energies. It is linearly expressed as:

$$q_e = \frac{RT}{b_T}\ ln\ K_T + \frac{RT}{b_T}\ ln\ C_e$$

b_T (J/mol) represents Temkin isotherm constant for sorption heat, K_T (L/g) is a parameter describing the highest binding energy while T (K) and R are temperature and gas constant, respectively.

A plot of q_e versus ln C_e yields slope and intercept used in the computation of the values of b_T and K_T.

4.6.2 Kinetics study

For an adsorption process, different mechanisms and factors control the rate of sorption of adsorbate on adsorbent and these include mass transfer and chemical process (Gautam et al., 2014). Therefore, to examine and validate the most probable mechanisms and potential rate-controlling stages, adsorption experimental data are tested by different kinetic models.

4.6.2.1 Pseudo 1st order

Linearized mathematical expression for the pseudo-first order is represented as:

$$\text{Log}\,(q_e - q_t) = log\,(q_e) - \frac{k_1}{2.303}t$$

q_e and q_t denote, respectively, the amounts of phenol adsorbed in mg/g at equilibrium and at time t (min). From slope and intercept of the plot of log (q_e-q_t) versus t, values of the rate constant k_1 and parameter q_e are obtained, respectively.

4.6.2.2 Pseudo 2nd order

Adsorption data are fitted on pseudo-second order model based on the linear algebraic equation:

$$\frac{t}{q} = \frac{t}{q_e} + \frac{1}{k_2}{q_e}^2$$

where q and qe denote the amounts of phenol or cadmium adsorbed (mg/g) by GPDADMAC or GPHM at time t (min) and at equilibrium. The slope and intercept of a plot of t/q against t give the equilibrium rate constant k_2 and parameter q_e.

4.6.2.3 Intraparticle diffusion

The weber's intraparticle diffusion kinetic form assumes that adsorption rate is limited by the adsorbate movement from the adsorbate surface to the intraparticle binding sites. This model is given by the following equation:

$$q_t = C_i + k_{id} \times t^{1/2}$$

The slope and intercept of the plot of q_t versus $t^{1/2}$ at stage i give k_{id} (the rate constant) and C_i (the model constant).

4.6.3 Thermodynamics

Inherent energetic changes during adsorption process are obtained from thermodynamic models through the variables of entropy change (ΔS), enthalpy change (ΔH) and Gibbs free energy change (ΔG).

Isosteric enthalpy change indicates if an adsorption process is exothermic or endothermic and it is obtained from the derivative Van't Hoff's expression (Inyinbor et al., 2016).):

$$ln\ K_o = \frac{\Delta S}{R} - \frac{\Delta H}{RT}$$

$$K_o = \frac{q_e}{C_e}$$

where K_o (g/L) is the distribution coefficient of adsorbate in solution, ΔH (J/mol) is the isosteric adsorption enthalpy change while T (K) and R are the absolute temperature and the ideal gas constant (8.314 J/mol K), respectively. A graph of $ln\ K_o$ against T^{-1}gives the value of ΔH. It follows that an exothermic adsorption process has a negative ΔH while an endothermic adsorption process has a positive ΔH. A magnitude of ΔH less than 50 kJ/mol implies physisorption process.

Also, the degree of orderliness of adsorbate molecules on adsorbent surface is measured by the adsorption entropy (ΔS) (J/mol K) obtained through the same Van't Hoff's equation above. Adsorption process with negative value of ΔS is said to have an ordered arrangement of adsorbate molecules on the adsorbent surface. In order words, the adsorbed

adsorbate molecules have restricted mobilities on the adsorbent surface as compared to the adsorbate molecules in the bulk solution.

The Gibbs free energy change describes the spontaneity of an adsorption process. It is calculated from the following equations:

$$\Delta G = -RT\ ln\ K_o$$

A negative and a positive ΔG (kJ/mol) means a spontaneous and a nonspontaneous adsorption process, respectively.

4.7 Regeneration Procedure

It is essential to investigate the number of times the adsorbents can be reused. For this purpose, regeneration study was conducted for both GPDADMAC and GPHM. DI water was used to wash GPDADMAC several times until no phenol was detected in the wash water by the UV-VIS spectrophotometer. Thereafter, it is air-dried in fume hood. Regarding GPHM, it was washed severally with 5 % HNO_3 until no cadmium was detected in the wash solution by the ICP-MS. Thereafter, the acid washed GPHM was rinsed several times to remove any trace of HNO_3. Then, it was air-dried in the fume hood.

4.8 Analytical measurement

The initial and final concentrations of phenol was measured using UV-VIS spectrophotometer (SPECORD-50, Analytic Jena) at 271nm wavelength following the method used by Roig, Gonzalez and Thomas, (2003). The calibration of the UV spectrophotometer was done using prepared standards of phenol concentration ranging

between 0 and 100mg/L. A linear calibration curve of absorbance against phenol concentration with R^2 equal 0.999 was obtained.

The concentrations of cadmium before and after the experiments were determined using ICP-MS (Thermo-Fischer Scientific). It uses argon gas (>99 % purity) for normal plasma generation and helium (>99% purity) for kinetic energy discrimination (KED) mode.

CHAPTER 5

RESULTS AND DISCUSSION

5.1 Adsorption of Phenol by GPDADMAC

5.1.1 Characterization of GPDADMAC

5.1.1.1 Surface Area and Pore Size Analyses

Textural properties of GPDADMAC were investigated by applying the N_2-physisorption analysis. The BET isotherm plot and the pore size distribution are presented in Figs. 5.1 (a and b, respectively). Following the IUPAC classification of adsorption isotherms (Zhang et al., 2016), GPDADMAC isotherm plot is similar to type II, which is characterized by uniform surface energy and multilayer adsorption. As suggested by its nitrogen uptake at low relative pressure range of 0 – 0.027, GPDADMAC has a microporous structure with monolayer physisorption. Furthermore, the change in adsorption from monolayer to multilayer approximately occurs at the relative pressure range of 0.027 - 0.32. There is a slow increase in the amount of nitrogen adsorbed at pressure range of 0.32 - 0.82 which is an indication of occurrence of both multilayer adsorption and condensation process. The sharp increase in nitrogen adsorption from relative pressure of 0.82 until saturation at 1 is indicative of presence of macropores in GPDADMAC. The Type H3 hysteresis loop at a relatively high pressure range indicates the mesoporous structure of GPDADMAC. Summing up, there is an indication that the pore system of GPDADMAC is characterized by micropores, mesopores and macropores.

Table 5.1 gives a summary of other parameters obtained from the analysis. The BET surface area of GPDADMAC was 357.4 m²/g which is higher than that of GO and other similar nanoadsorbent such as CNT (Li et al., 2013). Meanwhile, the pore size distribution as shown in Fig. 5.1b indicates that GPDADMAC has a size that falls within the range of 2–50 nm, confirming the preponderance of mesopores in the material. This may allow the phenol to have access to the inner layers of GPDADMAC.

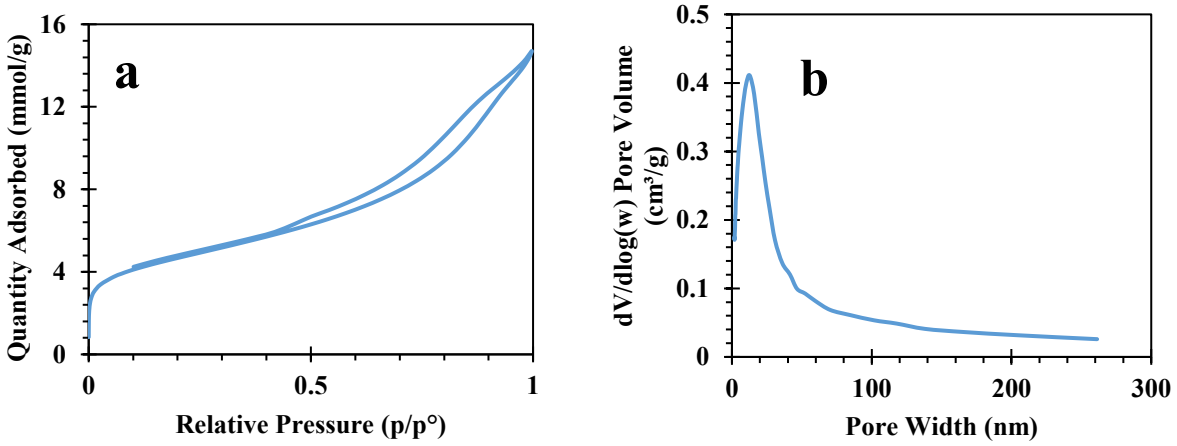

Figure 5.1: (a) Nitrogen sorption isotherm plot and (b) Pore size distribution curve for GPDADMAC

5.1.1.2 SEM and EDXS Analyses

Fig. 5.2 is the scanning electron microscopy (SEM) image of GPDADMAC which reveals a porous network with a fluffy sponge-like structure in contrast to the compact layer structure GO reported by Soleimani, Tehrani and Adeli, 2018). The loose sponge-like structure can be as a result of the attachment of PDADMAC to the GO surface. This kind of structure increases the volume and also the area of GPDADMAC which may play a significant role in increasing the adsorption of phenol. More than 50 % of the particle was of the size 3.2 nm which means that GPDADMAC is a nanomaterial.

Concerning the surface elemental composition of GPDADMAC, the EDXS spectrum in Fig. 5.3 shows that carbon, oxygen and nitrogen are the main elements within the spots inspected. Table 5.2 presents the average apparent concentration of each element. Compared to the EDX spectrum of graphene oxide reported by Şinoforoğlu et al., 2013, the presence of nitrogen can be inferred to come from the PDADMAC molecule and this can indicate that the graphene oxides were successfully functionalized by PDADMAC. The unidentified peak most probably emanated from the gold coating used to prepare the sample.

Table 5.1: Parameters of Nitrogen sorption analysis for GPDADMAC

Parameters	**Values**
Surface Area (BET)[a]	357.4 m^2/g
External Surface Area [b]	290.5 m^2/g
Micropore and Mesopore volume [c]	0.4579 cm^3/g
Micropore volume [b]	0.0357 cm^3/g
Mesopore and Macropore Volume [d]	0.4422 cm^3/g
Mesopore Volume	0.4221 cm^3/g
Macropore Volume	0.0201 cm^3/g
Average pore diameter [a]	51.25 Å

[a] obtained by BET.

[b] obtained from the t-plot.

[c] taken from the quantity of nitrogen adsorbed at about $P/P_0 = 0.95$.

[d] by BJH

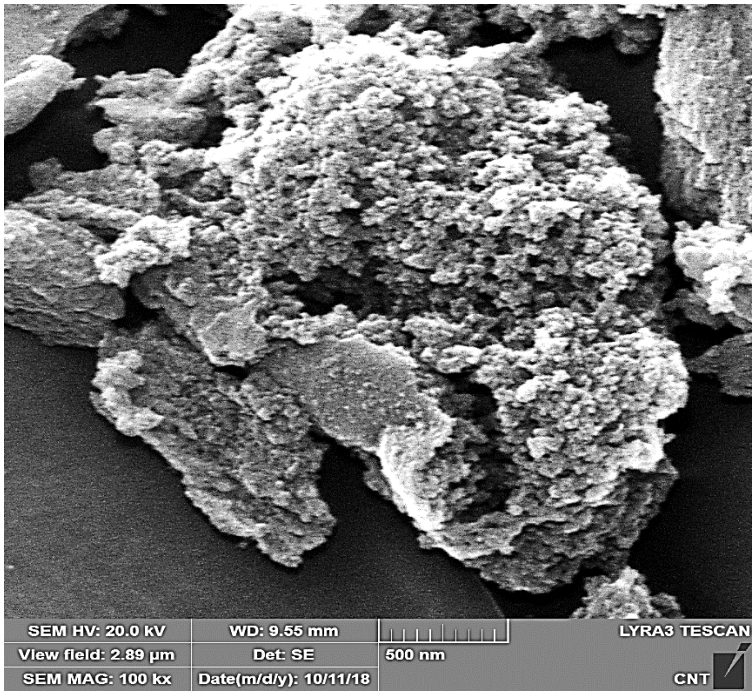

Figure 5.2: SEM image of GPDADMAC

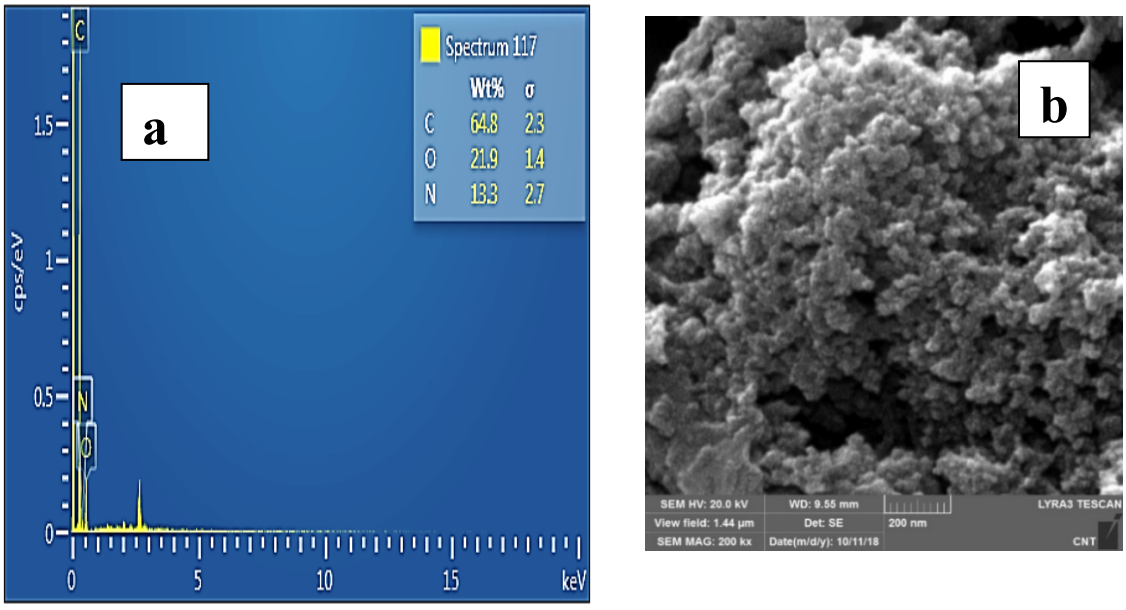

Figure 5.3: EDX Spectrum of GPDADMAC

Table 5.2: Elemental compositions by EDX

Element	Apparent Concentration (%)	Standard Deviation	k Ratio	Atomic weight (%)
C	40.98	4.87	0.47064	64.81
N	6.35	1.06	0.01076	13.32
O	6.30	1.24	0.02675	21.87
Total:				100.00

5.1.1.3 FTIR Analysis

Fig. 5.4 depicts the IR spectra of GO and GPDADMAC. It was observed that GO surface has oxygen functional groups as evidenced by hydroxyl groups at ~3441 cm^{-1}, a carboxyl group at ~1730 and ~1381 cm^{-1} as well as an epoxy group at ~838 and ~1154 cm^{-1}. The IR spectrum of GPDADMAC showed some modifications in the form of shifts, decrease and complete disappearance as well as the appearance of new IR peaks when compared to that of GO.

There is a downward shift of the peaks attributed to hydroxyl group from ~3441 in GO to ~3416 cm^{-1} in GPDADMAC; carboxyl group from ~1729 to ~1716 cm^{-1}; aromatic ring from ~1623 in GO to ~1609 cm^{-1} in GPDADMAC; upward shift of carboxyl group from ~1026 to ~1028 cm^{-1} and unattributable peaks from ~759 to ~785. There is also an increase in the intensity of the peak attributed to alkyl group at ~2920 cm^{-1} and disappearance of CN group peak at ~1259 cm^{-1} and unattributable peak at ~1454 cm^{-1}. This suggests that the interactions of GO and PDADMAC bring about reduction or modification of activities

of vibrational modes in the mixture (Yang et al., 2005). The disappearance of epoxy group peaks at ~838 and ~1154 cm^{-1} and carboxyl group peaks at ~1381 cm^{-1} in GPDADMAC indicates the reduction in the number of oxygen functional groups of GO (Ţucureanu et al., 2016). Meanwhile, the appearance of the characteristic peaks of PDADMAC in GPDADMAC, such as CHn group between ~2918 - ~2850 cm^{-1}, C=C group at ~1609 cm^{-1}, NO group at ~1383 cm^{-1} and CN group at ~1150 cm^{-1}, indicates that GO was successfully functionalized with PDADMAC. The results are similar to those reported by Ding et al., 2014; Li et al., 2016; Li et al., 2017; Huang et al., 2012 and Coates, J. (2000).

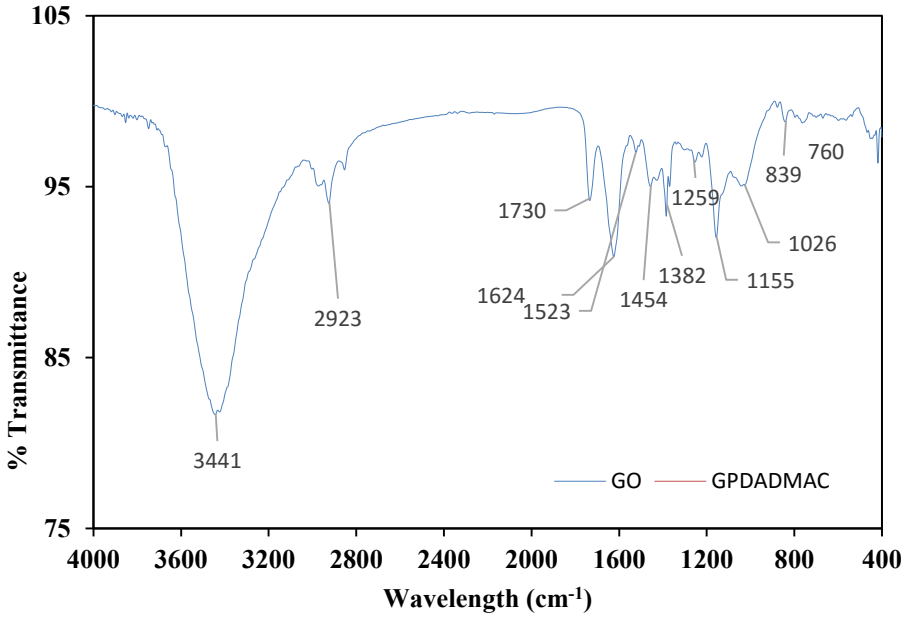

Figure 5.4: FTIR Spectra of GO and GPDADMAC

Table 5.3: Functional Group Attributions of IR peaks of GO and GPDADMAC

GO	GPDADMAC	ATTRIBUTIONS	DESCRIPTION
3443.74	3421.88	ν(O-H)	OH groups from C–OH group or water molecule
2925.37	2920.61- 2851.03	ν(CHn)	
1733.85	1719.68	ν(C=O)	Carboxyl -COOH group
1624.49		ν(C=C)	aromatic ring
	1612.43	δC=C	
1522.88	1524.45	?	
1457.36		?	
	1459.78	N-C	
1385.02		ν(C=O)	Carboxyl -COOH group
	1384.39	NO	Nitroso group
1254.20		δ(CN)	amide III (–CO–NH–) group
	1226.30	C-O-C	Epoxy group
1156.49		ν(C–O–C)	Epoxy
	1157.20	C-N	
1043.08	1034.54	ν(C-O)	Carboxyl group
842.69		δ(C–O–C)	Epoxy group
764.37	784.70	?	

ν means Stretching

δ means Bending or deformation

5.1.2 Removal of Phenol from Water

5.1.2.1 Effect of pH

As contained in various reports, initial solution pH affects the adsorbent surface charge, its functional group dissociation as well as adsorbate molecular structure, ionization and speciation. This makes the investigation of effect of pH on adsorption very crucial.

The investigation of phenol adsorption by GPDADMAC was carried out within the pH range of 3 to 10 by fixing adsorbent dosage at 4 g/L, initial concentration of phenol at

10ppm, agitation speed at 150rpm, temperature at 298 K and contact time at 30min. As shown in Fig. 5.5, the removal percentage of phenol by GPDADMAC increased from 62% to 79% as the pH was raised from 3 to 4. However, there was no additional removal of phenol as pH increased 4 to 9. Thereafter, a decrease in removal efficiency was noticed from pH 9 to 10. This trend is similar to that reported by Abdelwahab et al., (2013).

The PZC of GPDADMAC was measured to be 3.5. This means that the material surface is positively charged below 3.5 while it is negatively charged above 3.5. Lower removal efficiency recorded at pH 3 can be due to abundant positive charges on GPDADMAC surface resulting in static repulsion forces. On the other hand, since phenol exists as neutral molecules below its pKa of 10 and GPDADMAC is negatively charged at any pH value above 3.5 (PZC), therefore, it is possible that the removal of neutral phenol molecules within pH of 4 to 9 is due to the existence of dispersive interactions between the aromatic ring of phenol and the basal planes of GPDADMAC replenished with a high pi-electron density (Smets et al., 2016). The fairly constant removal efficiency at the pH range of 4 – 9 can be an indication of the PDADMAC coating stabilizing and reducing the rolling-up of the graphene in aqueous solution (Bolto and Gregory, 2007; Liu et al., 2016). Meanwhile, the fall in removal efficiency above pH 9 can be attributed to the repulsive forces between phenolate anions ion and the negatively charged surface of GPDADMAC.

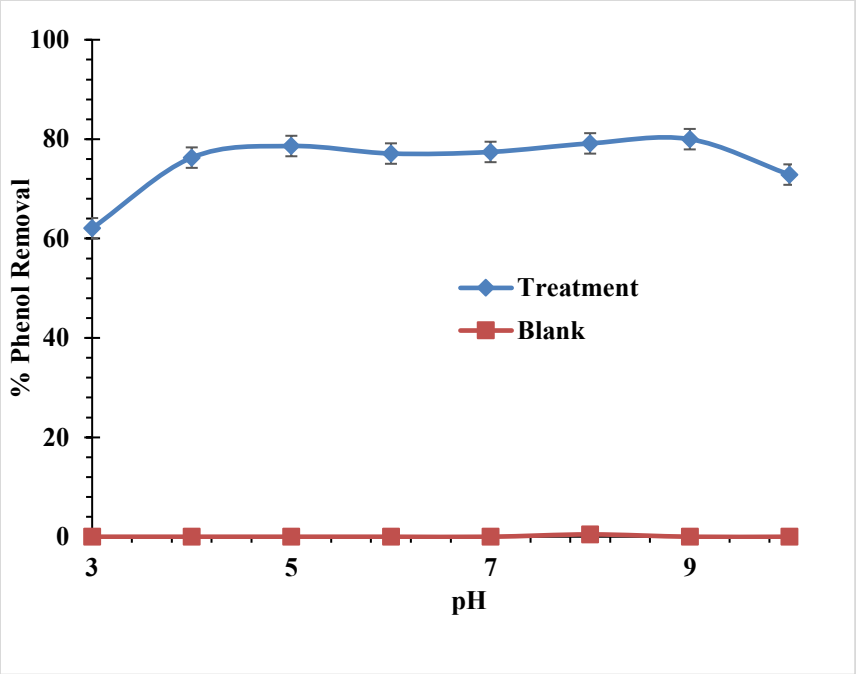

Figure 5.5: Effect of pH on phenol removal (initial conc. of phenol = 10 ppm, adsorbent dosage = 200 mg, agitation speed = 150 rpm, temperature = 298 K and contact time = 30 min)

5.1.2.2 Effect of Agitation Speed

As a factor influencing adsorption rate, agitation speed influences the attachment of the adsorbate ions to the adsorption sites of adsorbents (Asmaly et al., 2015). To this end, the impact of change in agitation speed on the removal of phenol by GPDADMAC was studied from 100 rpm to 250 rpm with other experimental conditions fixed at 10 ppm for initial phenol concentration, 4 g/L for adsorbent dosage, 298 K for temperature, 30 min for contact time and pH 6.

From Fig. 5.6 the percentage phenol removal by GPDADMAC slightly increased from 84% to 90% as the agitation speed was raised from 100 rpm to 150 rpm, which can be attributed to the improved contact between phenol molecules and adsorption sites of GPDADMAC (Asmaly et al., 2015). However, the removal efficiency remained almost

constant between 150 rpm and 200 rpm, which is an indication of saturation of the adsorption sites of GPDADMAC by phenol molecules. A further increase of agitation speed from 200 to 250 rpm resulted in a decrease in percentage removal of phenol. This observation can be as a result of random collisions between particles (adsorbent–adsorbent, adsorbent–adsorbate and adsorbate–adsorbate) which did not provide enough time to the phenol to make a bond with surface of the GPDADMAC.

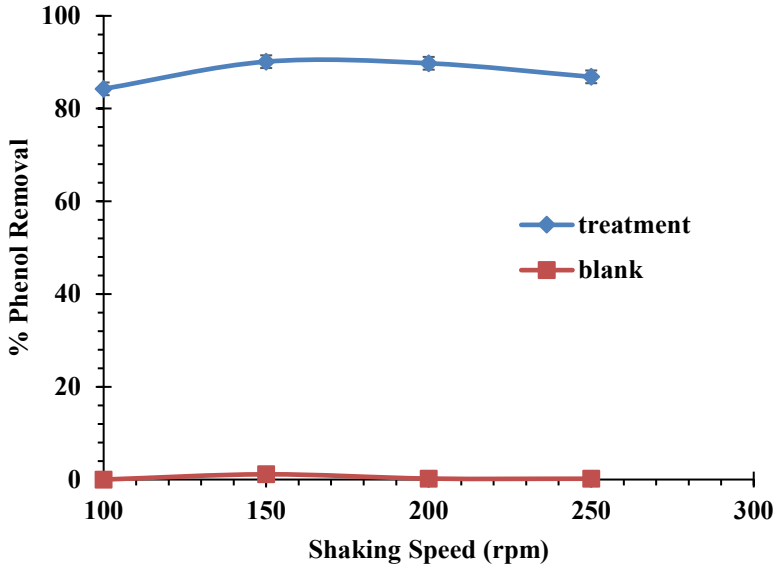

Figure 5.6: Effect of agitation speed on phenol removal (initial conc. of phenol =10ppm, adsorbent dosage = 200mg, temperature = 298 K, contact time = 30min and pH = 6)

5.1.2.3 Effect of temperature

At constant experimental conditions of 10 ppm initial phenol concentration, 4g/L adsorbent dosage, 150 rpm agitation speed, pH 6 and contact time of 30 min, the influence of various temperature levels (15 ºC, 25 ºC, 35 ºC and 45 ºC) on phenol adsorption by GPDADMAC was studied. A slightly lower removal efficiency is observed at temperatures immediately lower than 25 ºC. Also, an increase in temperature from 25 ºC results in a decrease in the

amount of phenol adsorbed by GPDADMAC (Fig. 5.7). This can be due to an increase in average kinetic energy of phenol molecules resulting from increased temperature which leads to disturbance of the stability of the phenol- GPDADMAC complex and thereby causing desorption instead of adsorption (Alinnor and Nwachukwu, 2011).

It can also be inferred that phenol adsorption by GPDADMAC is exothermic and also that the best performance of GPDADMAC for phenol removal can be obtained at room temperature.

5.1.2.4 Effect of Adsorbent Dosage

The influence of GPDADMAC dosage from 25 mg to 200 mg, as shown in Fig. 5.8, was studied under the prevailing experimental conditions fixed at initial concentration of phenol of 10ppm, contact time of 30 min, temperature of 298 K, pH of 6 and agitation speed of 150 rpm. It was observed that an increase in adsorbent dosage leads to a rise in phenol removal. A significant rise from 30% at 25 mg to 79% at 200 mg was observed as the dosage increased.

The observation can be associated with availability of increasing number of adsorption sites when the amount of adsorbents was increased (Anbia and Ghaffari, 2009; Asmaly et al., 2015). However, it can also be noticed that the removal percentage was increasing in a gradual pattern due to the fact that the number of phenol molecules remaining in the solution for adsorption by further increased dosage kept decreasing. In other words, the adsorption is tending towards equilibrium between phenol molecules adsorbed on the GPDADMAC and the un-adsorbed phenol molecules in the aqueous medium as dosage increased (Asmaly et al., 2015)

5.1.2.5 Effect of initial concentration

Fig. 5.9 presents the observed changes in adsorption of phenol by GPDADMAC at different initial concentration of phenol. Initial concentration of 5 ppm, 10 ppm and 20 ppm were examined under other constant experimental parameters of 4 g/L adsorbent dosage, room temperature, 30 min contact time, 150 rpm agitation speed and pH 6. As the initial concentration increases from 5 ppm to 20 ppm, the removal percentage of phenol decreases from more than 90% to about 80%.

The presence of large number of phenol molecules provided by the increasing initial concentration as opposed to the limited fixed adsorption sites on GPDADMAC may be responsible for the observed phenomenon. This means that there will be more vacant adsorption sites, which can take up more phenol ions at lower initial concentration. However, these vacant sites become occupied by phenol ions as initial concentration increases until saturation. Thus, the adsorption sites needed to attach the increased phenol concentration will not be available and hence the resulting decrease in adsorption rate (Asmaly et al, 2015; Dolaksiz, Temel and Tabakci, 2018).

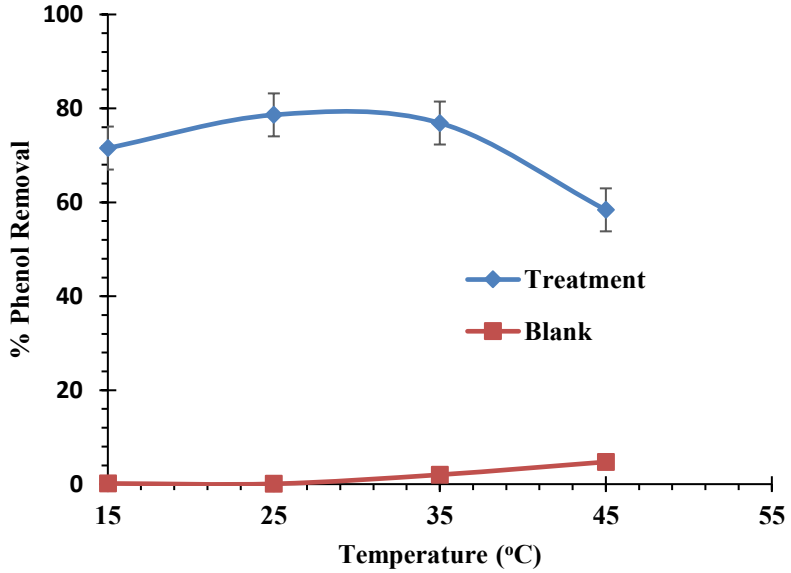

Figure 5.7: Effect of temperature on phenol removal (pH = 6, initial conc. of phenol =10 ppm, adsorbent dosage = 200 mg, contact time = 30 min and agitation speed= 150 rpm)

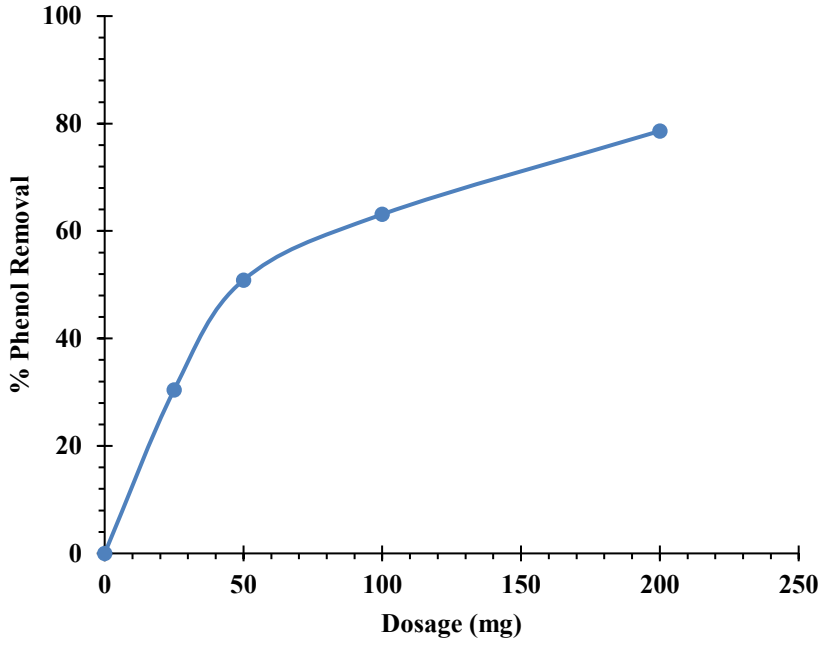

Figure 5.8: Effect of GPDADMAC dosage on phenol adsorption (initial phenol conc. =10 ppm, contact time = 30 min, agitation speed = 150 rpm, temperature =298 K and pH = 6)

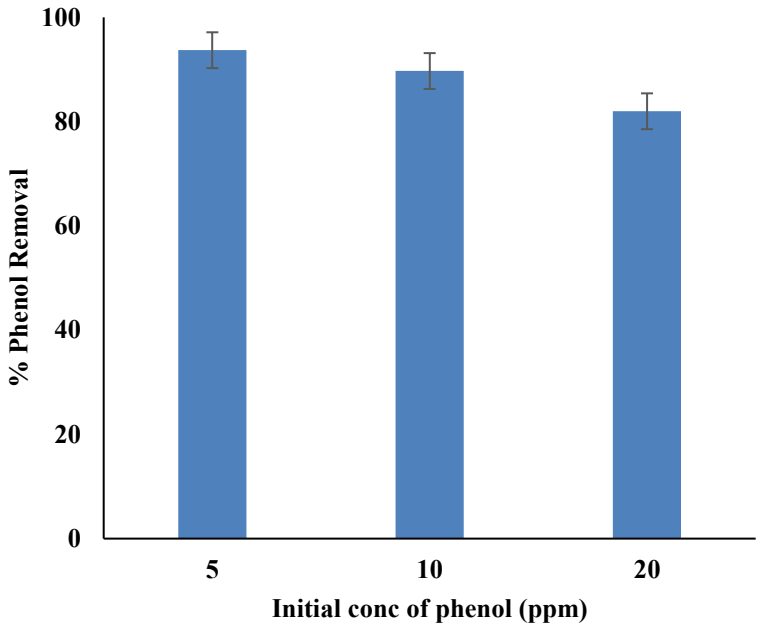

Figure 5.9: Effect of phenol initial concentration on removal efficiency (pH = 6, agitation speed = 150 rpm, temperature =298 K, adsorbent dosage = 200 mg and contact time = 30 min)

5.1.2.6 Effect of Contact Time

The investigation is important for establishing the equilibrium state at which the concentration of adsorbate remains relatively constant after some definite period of time in an adsorbate-adsorbent medium.

Fig. 5.10 depicts the effect of contact time on adsorption of phenol by GPDADMAC, which was obtained under varying time of 1 to 30 minutes and other experimental conditions set at adsorbent dosage of 4 g/L, initial concentration of phenol of 10 ppm, agitation speed of 150 rpm, temperature of 298 K and pH 6.

Obviously, GPDADMAC is a super-fast adsorbent for phenol removal from aqueous medium. The removal of phenol by GPDADMAC was very quick within the first 5 minutes with about 78% phenol removal efficiency. However, its phenol removal efficiency

became gradual beyond 5 min until equilibrium was reached at about 10 min wherein about 86% of phenol was removed by GPDADMAC.

The exceptional initial fast adsorption rate observed within the first 5 minutes may have resulted from the huge surface areas conferred on the graphene by the PDADMAC forming a fluffy sponge-like structure, which allowed accumulation of many phenol molecules. In addition, the observed high initial adsorption rate can also be as a result of availability of hydrophobic cavities formed from the opposite orientation between the cluster of ionic parts and the cluster of hydrophobic parts of the PDADMAC monomer units which houses sparingly soluble phenol molecules. Meanwhile, the spaces in the fluffy sponge-like structure and hydrophobic cavities are reduced with time as most of them were already being occupied by phenol molecules, thereby resulting in slow adsorption rate observed between 5 and 10 min. Eventually, when they were completely saturated with phenol molecules around 10 minutes, the equilibrium was reached with 86 % phenol removal (Yu et al., 2017). Therefore, the optimum contact time was chosen to be 10 min.

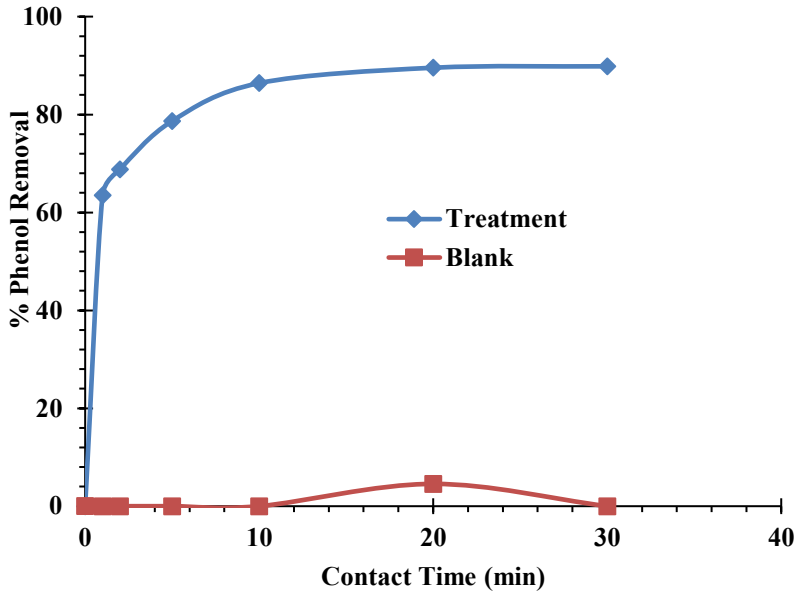

Figure 5.10: Effect of contact time on phenol adsorption (initial phenol conc. = 10 ppm, adsorbent dosage = 200 mg, agitation speed = 150 rpm, Temperature = 298 K, and pH = 6)

5.1.3 Kinetics, Isotherms and Thermodynamics

5.1.3.1 Kinetics study

Adsorption data are fitted into pseudo first order, pseudo second order and intra particle diffusion kinetic models.

The value of the rate constant k_1 and parameter q_e for the pseudo first order model, as contained in Table 5.4, were calculated from the slope and the intercept of the graph of log (q_e-q_t) against t shown in Fig. 5.11a. The relatively low value of R^2 (0.9221) is an indication that pseudo-first order model did not well represent phenol adsorption on GPDADMAC. Fig. 5.11b displayed the fit of the adsorption data on pseudo-second order model. Values of equilibrium rate constant k_2 and parameter q_e, also provided in Table 5.4. The resulting fitted straight line gives an indication that pseudo-second order model well represents the

adsorption process. Moreover, the high value of R^2 (0.9994) and the similarity between the calculated q_e and experimental q_e further support the validity of the model for phenol adsorption by GPDADMAC. It implies that the adsorption of phenol on GPDADMAC is most likely to be monolayer with chemical processes controlling the adsorption rate.

As shown in Fig. 5.12, the weber's intraparticle diffusion model is characterized by multilinearity with three different stages. The first stage is the external surface adsorption wherein adsorbate ions are transported from the boundary film to the external surface of the adsorbate and this was completed within the first 4 min. The second stage at which intraparticle diffusion is a limiting factor to the adsorption process was observed in less than 10 minutes. The intraparticle diffusion started declining in the third portion of the plot. The multilinearity of the model as well as the deviation of the trend lines of the three stages from the origin mass transfer difference between the first and last stage suggest that the adsorption is not only limited by intraparticle diffusion.

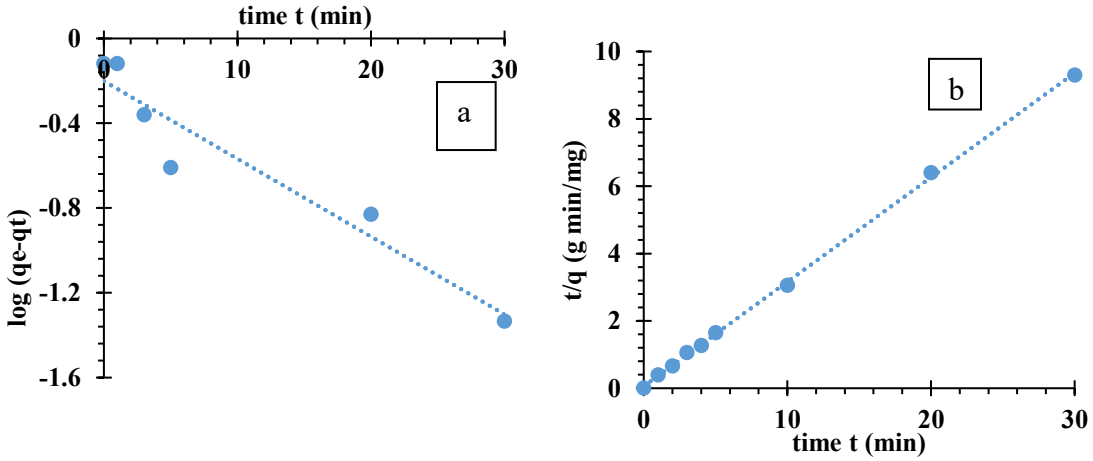

Figure 5.11: (a) Pseudo-first order (b) Pseudo-second order (pH = 6, agitation speed =150 rpm, room temperature, adsorbent dosage = 4 g/l and initial phenol conc =20 mg/l)

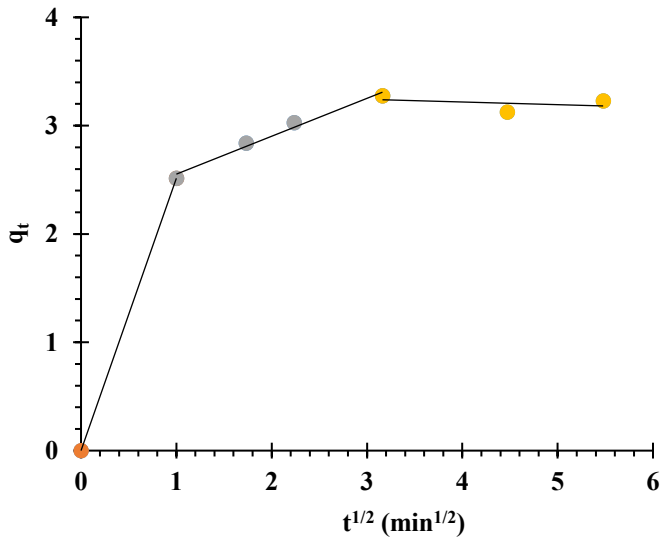

Figure 5.12: Intraparticle diffusion model (initial phenol conc. =20 mg/l, GPDADMAC dosage = 4 g/l, agitation speed =150 rpm, temperature = 296 K, pH = 6)

Table 5.4: Kinetic models for the adsorption of phenol by GPDADMAC

Kinetic model	**Parameters**	**Value**
Pseudo-first-order	q_e (mg/g)	0.6297
	k_1 (min^{-1})	0.0845
	R^2	0.9221
	q_e experimental (mg/g)	1.65
Pseudo-second-order	q_e (mg/g)	3.224
	k_2 (g/(mg min)	1.6494
	R^2	0.9994
	q_e experimental (mg/g)	1.65
Intraparticle diffusion	k_1 (mg/g $min^{-1/2}$)	2.5138
	R^2	1.0
	k_2 (mg/g $min^{-1/2}$)	0.35
	R^2	0.9823
	k_3 (mg/g $min^{-1/2}$)	-0.0246
	R^2	0.1422
	q_e experimental (mg/g)	1.65

5.1.3.2 Isotherm Models

To describe the type of interactions between phenol molecules and GPDADMAC which is responsible for its adsorption, experimental data were fitted on isotherm models. Figs. 5.13, 5.14 and 5.15 show the plots of Langmuir, Freundlich and Temkin isotherm models, respectively while Table 5.5 gives the summary of the parameters of the three models.

As it can be observed in Table 5.5, the Langmuir and Temkin models show a good fit with correlation coefficients greater than 0.99, which means that the adsorption of phenol molecules by GPDADMAC can be explained by the two models. Based on the Langmuir model in Fig. 5.13, it implies that there is a strong attachment of phenol molecules onto a limited number of adsorption sites with homogenous sorption energies present on a single surface layer of GPDADMAC. Furthermore, the value of separation factor, R_L, which is between 0 and 1, indicates that the adsorption of phenol on the GPDADMAC is favorable. The good fit shown by the adsorption experimental data on Temkin model in Fig. 5.15 indicates that increase in the surface coverage of GPDADMAC by phenol molecules leads to a linear decrease in the sorption energies. Moreover, the positive value of the constant, b, points to the fact that the adsorption process is exothermic.

Table 5.6 gives the comparison of the performance of GPDADMAC with other materials from literature.

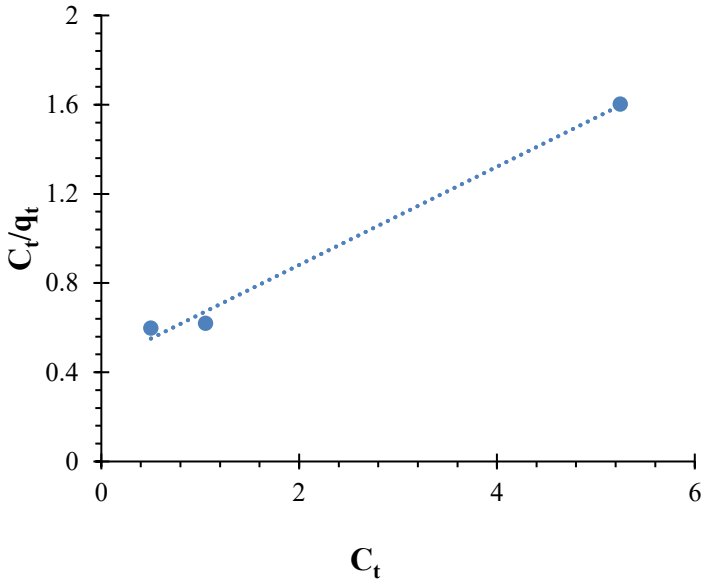

Figure 5.13: Langmuir Isotherm Plot

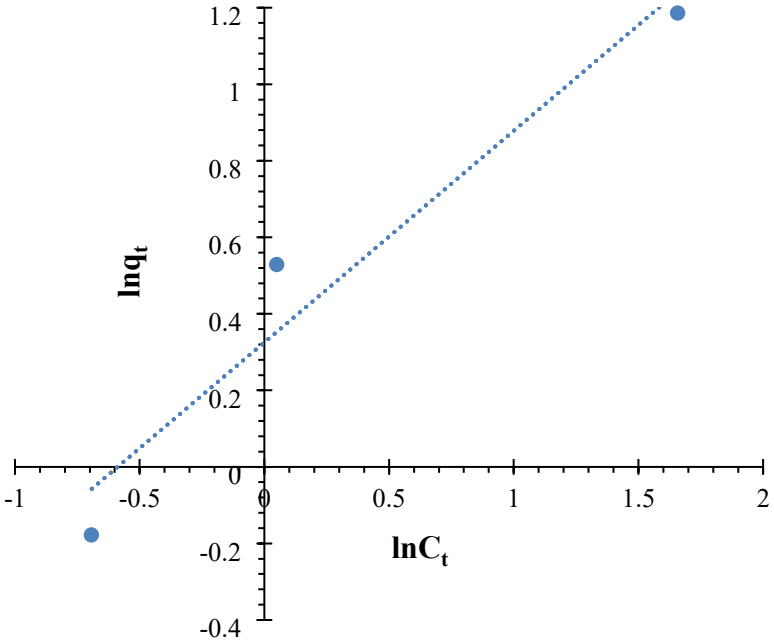

Figure 5.14: Freundlich Isotherm Plot

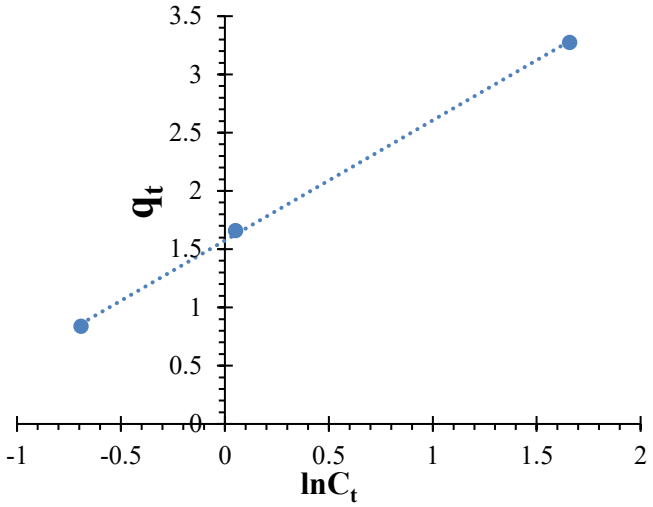

Figure 5.15: Temkin Isotherm Plot

Table 5.5: Parameters of Isotherm models

LANGMUIR	FREUNDLICH	TEMKIN
R^2 = 0.9924	R^2 = 0.9479	R^2 = 0.9995
K_L (L g^{-1}) = 0.4995	K_F (mg g^{-1}) = 1.3846	K_T (mg g^{-1}) = 4.595
q_m (mg g^{-1}) = 4.5413	n = 1.8086	b (J mol^{-1}) = 2400.5
R_L = 0.2096		

5.1.3.3 Thermodynamics

The thermodynamic model was investigated at absolute temperatures of 298 K (25 ºC), 308 K (35 ºC) and 318 K (45 ºC) under the experimental conditions of 10 ppm initial phenol concentration, 4 g/L adsorbent dosage, 30 mins contact time, 150 rpm agitation speed and initial solution pH of 6. From the plot of ln K_o versus T^{-1} displayed in Fig. 5.16, the enthalpy change (ΔH) and entropy change (ΔS) were, respectively, obtained from the slope and intercept. The free energy change (ΔG) was calculated from the equation:

$$\Delta G = -RT\ ln\ K_o$$

$$K_o = \frac{q_e}{C_e}$$

The values of (ΔH), (ΔS) and (ΔG) are summarized in Table 5.7.

Table 5.6: Comparison of performance of GPDADMAC with other materials from literature.

Material	**Adsorption capacity (mg g^{-1})**	**% Phenol Removal**	**Contact Time**	**Initial Phenol Concentration**	**Adsorbent dosage**	**Ref.**
activated carbon (AC)	1.348 (Langmuir Isotherm)	75%	2 hrs	2 mg L^{-1}	50mg	(Asmaly et al., 2015)
carbon nanotubes (CNTs)	1.098 (Langmuir Isotherm)	62%	2 hrs	2 mg L^{-1}	50mg	
fly ash (FA)	1.007 (Langmuir Isotherm)	60%	2 hrs	2 mg L^{-1}	50mg	
carbon nanofibers (CNFs)	0.842 (Langmuir Isotherm)	41%	2 hrs	2 mg L^{-1}	50mg	
Activated carbon from sawdust	0.022 (Langmuir Isotherm)	-	3 hrs	20 mg L^{-1}	10 g L^{-1}	(Meniai, 2012)
Graphene	18.6 (Experimental)	63.1%	48 hrs	50 mg L^{-1}	1.7 g L^{-1}	(Li et al., 2012)
GPDADMAC	4.5413 (Langmuir Isotherm	~ 90%	10 mins	10 mg L^{-1}	400 mg	This work

5.1.4 Regeneration Study of GPDADMAC

The adsorption efficiency of regenerated GPDADMAC was evaluated after two cycles of desorption with DI water. As shown in Fig. 5.17, a very drastic reduction in the removal efficiency was observed after the cycles of regeneration. The removal efficiencies after the

second and third cycles were found to be about 11% and 3%, respectively. This can be indicative of the interaction between phenol molecules and GPDADMAC being chemisorption. It is a further support for the observed fitness of the pseudo second order kinetic model and the difference in the FTIR spectra of GPDADMAC before and after adsorption.

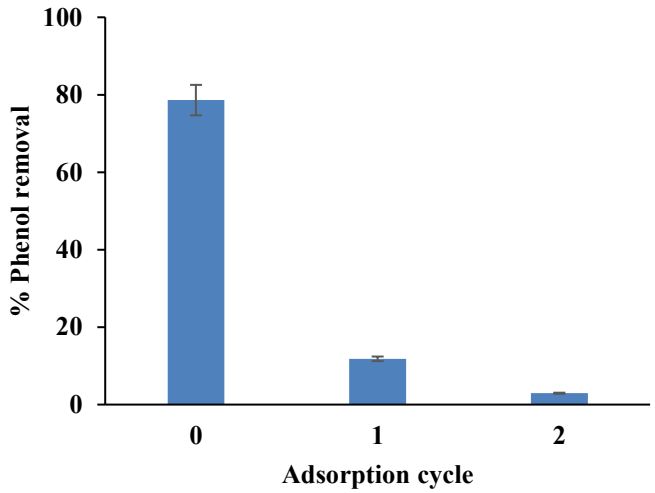

Figure 5.16: Removal efficiency of GPDADMAC for a number of adsorption/regeneration cycles (dosage = 4 g/l, initial concentration of phenol = 10 mg/l, temperature = 298 K, pH = 6, agitation speed = 150 rpm)

5.1.5 Treatment of phenol-spiked Groundwater

The adsorption efficiency of GPDADMAC and GPHM were tested for the removal of phenol and cadmium, respectively, in spiked real groundwater. The result of the anion-cation analysis is displayed in Table 5.8. The conductivity was measured to be 3436 µS/cm using multimeter . Also, the phenol and the cadmium concentrations in the groundwater were at undetecable level as measured by spectrophotometer and ICP-MS, respectively.

For the evaluation of the removal efficiency of GPDADMAC, the groundwater was spiked with 10 ppm of phenol. Without any pH adjustment and using other optimized conditions of adsorbent dosage of 4g/L, agitation speed of 150 rpm, temperature of 25 ºC and contact

time of 30 min, the removal efficency of GPDADMAC for phenol in real groundwater was 49% compared to 80% in synthetic water. The reduction in efficiency can be attributed to the precence of other ions in the groundwater which compete with phenol for the active sites of GPDADMAC.

Table 5.7: Characteristics of Groundwater before spiking

Cations (ppm)	**Anions (ppm)**
Sodium (Na) = 354.152	Fluoride (F) = 2.436
Potassium (K) = 10.619	Chloride (Cl) = 759.167
Magnesium (Mg) = 39.784	Bromide (Br) = 9.226
Calcium (Ca) = 102.907	Nitrate (NO_3) = 9.135
	Sulfate (SO_4) = 340.684
Conductivity = 3436 µS/cm Phenol concentration = ND Cadmium concentration = ND	

5.2 Adsorption of Cd by GPHM

5.2.1 Characterization of GPHM

5.2.1.1 Surface Morphological Analysis of GPHM (BET)

From the nitrogen physisorption curve in Fig. 5.18a, the isotherm curve shows similarity to type II adsorption curve of the IUPAC classification. This is obvious from the way the quantity adsorbed at low relative pressure sharply increases, which indicates the presence of micropores in the GPHM. As the relative pressure increases further, the initial sharp increase in adsorption is accompanied by a slow increase at the moderate relative pressure,

which is an indication of the availability of mesopores and, at the same time, pointing at a change from a monolayer adsorption to a multi-layer adsorption. When the relative pressure is close to 1, the adsorption sharply rises again, which is due to presence of well-developed macropores.

Fig. 5.18b, showing the distribution of pores in GPHM, suggests that the mesopores predominate in the adsorbent as it can be seen that the largest pore volume is occupied by the pore width between 2 -50 nm. Other parameters of the nitrogen adsorption-desorption analysis are summarized in Table 5.9. GPHM has a high BET surface area of about 198 m^2/g.

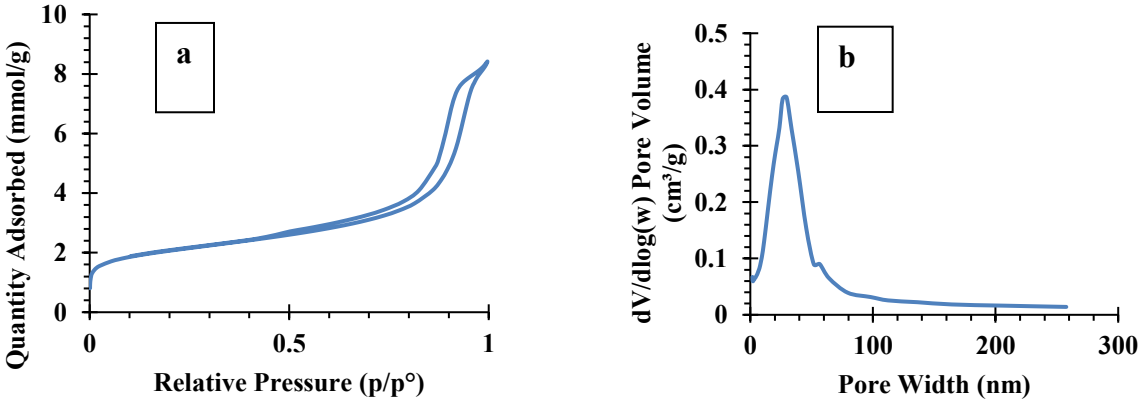

Figure 5.17: (a) Nitrogen adsorption-desorption isotherm curve at 77 K and (b) Pore size distribution curve for GPHM

Table 5.8: Parameters of Nitrogen sorption analysis

Parameters	Values
Surface Area (BET) [a]	198.36 m^2/g
External Surface Area [b]	128.74 m^2/g
Micropore and Mesopore volume [c]	0.2504 cm^3/g
Micropore volume [b]	0.0245 cm^3/g
Mesopore and Macropore Volume [d]	0.2532 cm^3/g
Mesopore Volume	0.2230 cm^3/g
Macropore Volume	0.0272 cm^3/g
Average pore diameter [a]	59.497 Å

[a] obtained by BET.

[b] obtained from the t-plot.

[c] taken from the quantity of nitrogen adsorbed at about $P/P_0 = 0.95$.

[d] by BJH

5.2.1.2 SEM and EDX Analyses

Fig. 5.19 (a and b) are SEM images of GPHM at 2 kx and 10 kx magnifications, respectively. A comparison of GPHM to GO reported by Pavoski et al. (2015) shows that the surface of the GO has been covered by some PHM. This can be seen clearly in Fig 5.19a. A deeper look on the surface of GPHM as shown in Fig 5.19b reveals that it exhibits a kind of wrinkled morphology. All these observations indicate that GO was successfully

functionalized with PHM. Similar reports were published by Kharismadewi et al., (2016) and Massoumi et al., (2016). The EDX spectrum (Fig. 5.20) shows that GPHM contains carbon and oxygen at apparent concentrations of 81.04% and 18.94%, respectively as given in Table 5.10.

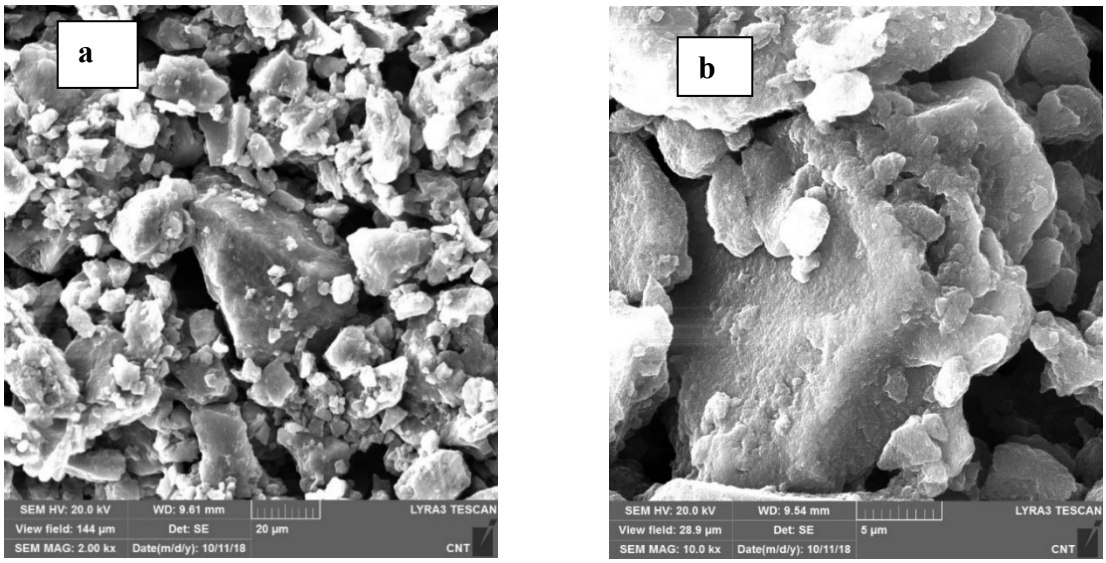

Figure 5.18: SEM images of GPHM at (a) 2000X and (b) 10000X

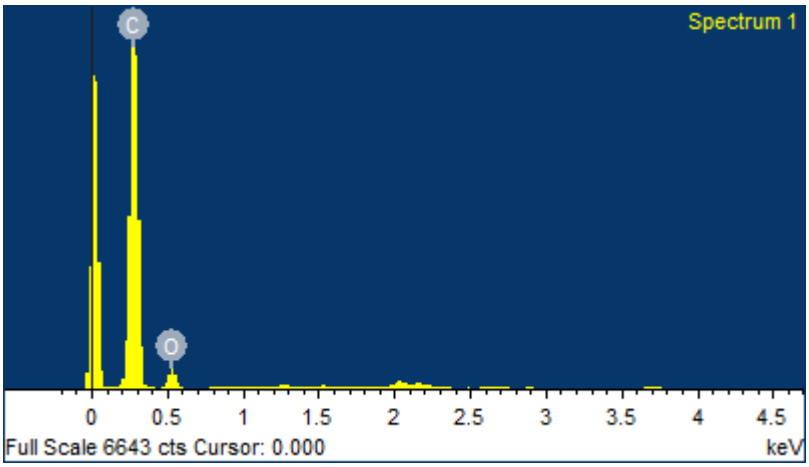

Figure 5.19: EDX spectrum of GPHM

Table 5.9: Elemental compositions by EDX

Element	**Apparent Concentration (%)**	**Atomic weight (%)**
C	81.04	85.06
O	18.96	14.94
Total:	100.00	100.00

5.2.1.3 FTIR Analysis

The FTIR spectrum of GPHM is shown in Fig. 5.21. The assignment of functional group to the peak at 3423 cm^{-1} reveals that it is most probably the strong and broad OH group from the polymer based 2-hydroxyethyl methacrylate (PHM) used for grafting the graphene. It is however possible for this broad OH group to have overlapped most of the aliphatic C-H groups peculiar to PHM (Massoumi et al., 2016). Other peaks which are indications that the PHM successfully functionalized the surface of GO are 1384 cm^{-1} for the bending vibrations of C-H and 1079 cm^{-1} for the stretching vibration of C-O-C. Some of the published works that have similar observations include Liu et al., (2015).

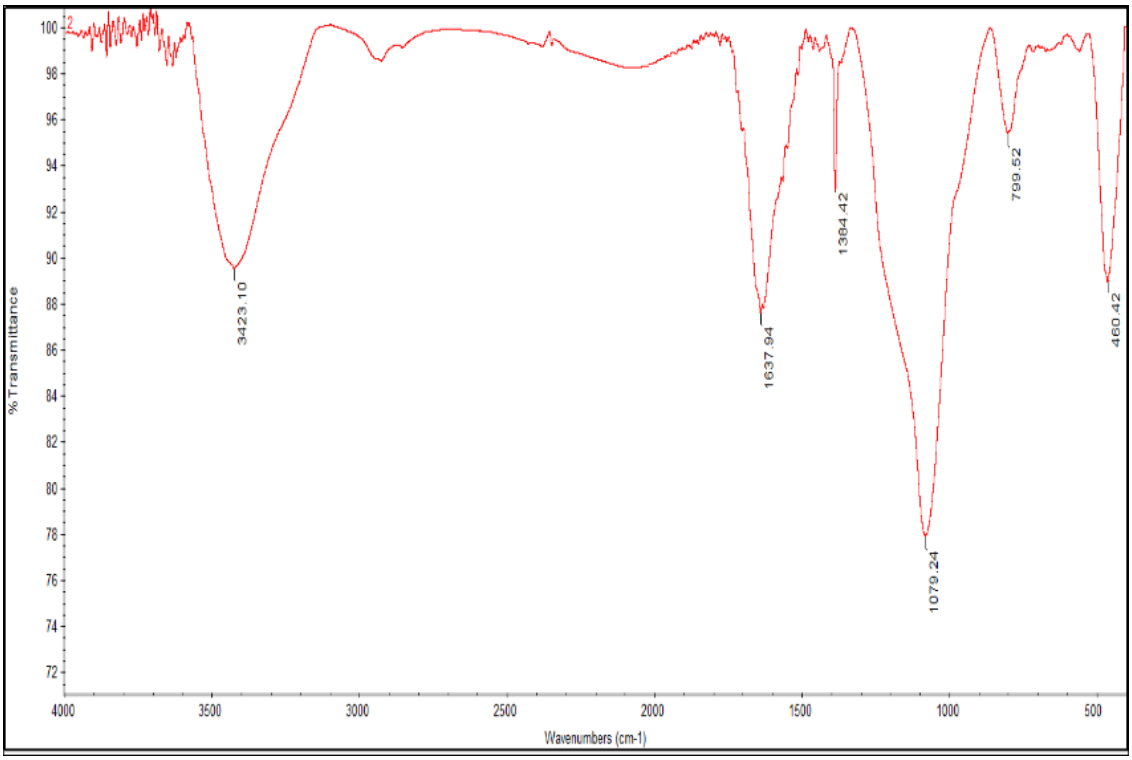

Figure 5.20: FTIR Spectrum of GPHM

5.2.2 Removal of Cadmium Ion by GPHM

5.2.2.1 Effect of pH

The influence of initial solution pH on adsorbent surface charge, its functional group dissociation as well as adsorbate molecular structure, ionization and speciation makes the investigation of effect of pH on adsorption very crucial. Moreover, adsorption of metals is greatly determined by the competition for the binding sites by them and hydrogen ions. The effect of pH on cadmium adsorption was studied under varying pH of 3, 5, 7 and 9. As it is apparent in Fig. 5.22, the percentage removal of cadmium increased from 20 % to 60% when the pH value rose from 3 to 7. Beyond pH of 7, there was a decrease in the percentage of cadmium adsorbed. At a lower pH of 3, the predominance of hydrogen ions in solution could have led to their more adsorption onto the active sites than are cadmium ions.

Maximum removal of cadmium was achieved when the pH was increased to 7. Beyond pH 7, the removal could be attributed to precipitation of cadmium as shown by the behavior of the blank. Arshadi, Amiri and Mousavi, (2014) reported a similar observation using barley straw ash as adsorbent.

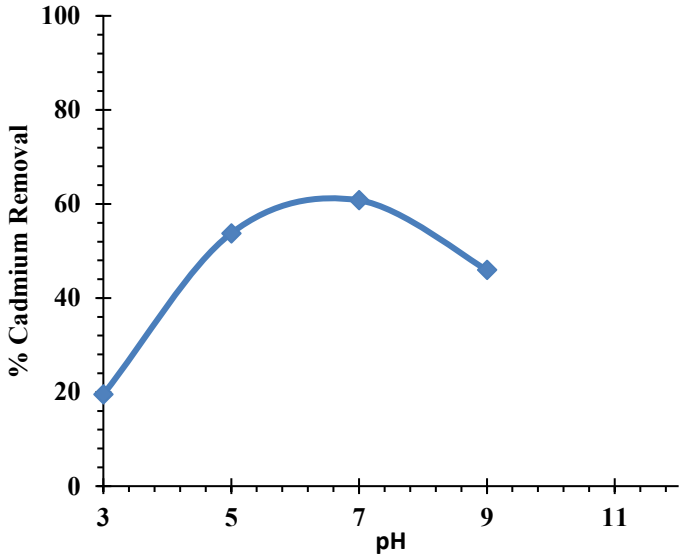

Figure 5.21: Effect of initial solution pH on cadmium removal (adsorbent dosage = 25 mg; initial cadmium concentration = 0.5 ppm; volume of solution = 50 ml; agitation speed = 200 rpm; temperature = 298 K; contact time = 30 min.)

5.2.2.2 Effect of agitation

Agitation speed is one of the factors that can affect adsorption rate as it influences the attachment of adsorbate on the adsorption sites of adsorbents. Fig. 5.23 depicts the obtained result of the effect of agitation speed on the removal of cadmium by GPHM. The removal efficiency increased when the agitation speed was raised from 100 rpm to 200 rpm. This was followed by decreased removal up to 250rpm. Highest adsorption of cadmium (~60 %) was observed at 200 rpm. The observed increase in removal efficiency from 150 rpm to 200 rpm may be due to the improved contact between the adsorbent binding sites and cadmium ions. Meanwhile, the decrease from 200 rpm to 250 rpm was likely to be caused

by the disturbance of already adsorbed cadmium ions which led to their desorption from the adsorbent active sites.

5.2.2.3 Effect of temperature

From Fig. 5.24, increase in temperature between 288 K and 298 K resulted in an increased removal efficiency of GPHM for cadmium. A further increase from 298 K (room temperature) resulted in lower adsorption of cadmium. Therefore, the maximum percentage removal of cadmium was approximately 60 % at 298 K. Al-Homaidan et al., (2015) reported a similar observation using *Spirulina platensis* dry biomass for cadmium adsorption.

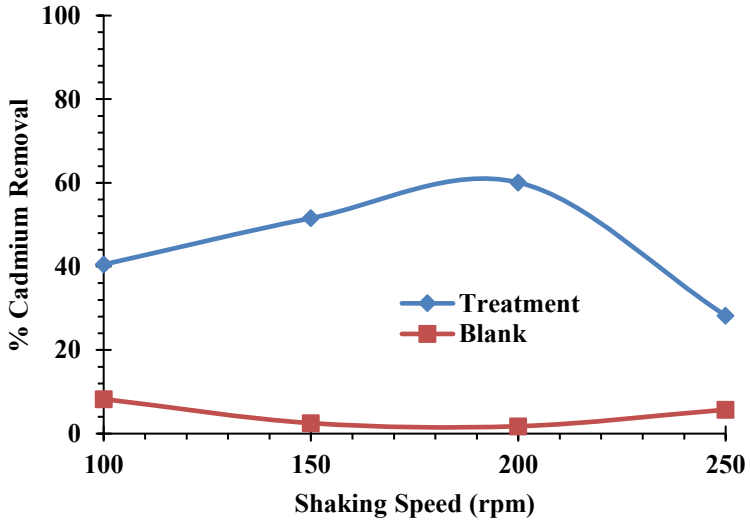

Figure 5.22: Effect of agitation speed on cadmium removal by GPHM (adsorbent dosage = 25 mg; initial cadmium concentration = 0.5 ppm; volume of solution = 50 ml; initial solution pH = 7; temperature = 298 K; contact time = 30 min)

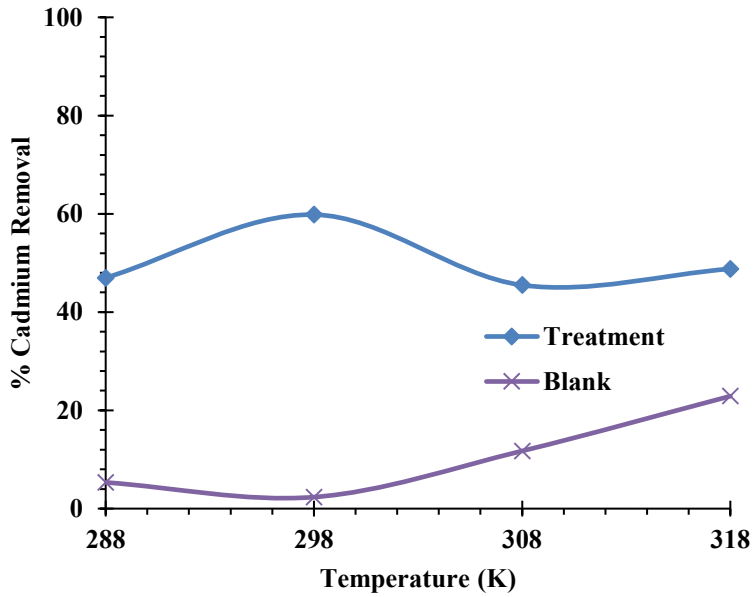

Figure 5.23: Effect of temperature on cadmium adsorption by GPHM (adsorbent dosage = 25 mg; initial cadmium concentration = 0.5 ppm; volume of solution = 50 ml; initial solution pH = 7; agitation speed = 200 rpm; contact time = 30 min)

5.2.2.4 Effect of dosage

Adsorbent dosage greatly affects the removal of heavy metals from aqueous medium because it influences the capacity an adsorbent has for a given initial adsorbate concentration at certain experimental conditions. The extent of influence of GPHM adsorbent dosage on cadmium removal was investigated for the dosage of 5 mg, 10mg, 20 mg and 25 mg under other fixed experimental conditions. As displayed in Fig. 5.25, the result revealed that percentage removal of cadmium rose from 60 % to 79 % when GPHM dosage was increased from 5 mg to 20. A further increase beyond 20 mg to 25 mg yielded an insignificant percentage removal of cadmium. Similar observation was reported in literature for the adsorption of cadmium by Al-Qahtani, (2017). The observed increase could be attributed to the presence of large surface area of the adsorbent when the dosage

was increased which provided more active binding sites for the attachment of cadmium ions.

5.2.2.5 Effect of initial concentration

Investigation of the impact of initial metal ion concentration on their adsorption is very necessary because it determines the driving force available to get over all resistances by mass transfer between the liquid and solid phase. Change in adsorption of cadmium was studied at various concentrations of 0.05 ppm, 0.1 ppm and 0.5 ppm. The percentage removal increased as the initial concentration changed from 0.05 ppm to 0.1 ppm until it attained maximum of about 70 % at a concentration of 0.5 ppm (Fig. 5.26). There was no significant increase between 0.25 ppm and 0.5 ppm. The obtained results are well-matched to Ehrampoush et al., (2015). The rise in removal percentage as the initial concentration increased could be that not all the active sites were occupied at lower concentration of cadmium. When all the active sites were almost saturated at 0.1 ppm, the removal percentage was almost plateau until 0.5 ppm.

5.2.2.6 Effect of contact time

Experiment was conducted to study the effect of various contact time, ranging from 0 to 30 min, on the removal of cadmium ions by GPHM. As shown in Fig. 5.27, the removal percentage was observed to be fast within the first 6 min. After this time, there was a slow increase in removal. There was no considerable change in the percentage removal from 20 min to 30 min. The fast and high removal at the initial contact time can be due to the availability of numerous vacant active sites on the adsorbent and also more cadmium. As time passed, most vacant binding sites became occupied with cadmium ions which resulted in the stable removal efficiency.

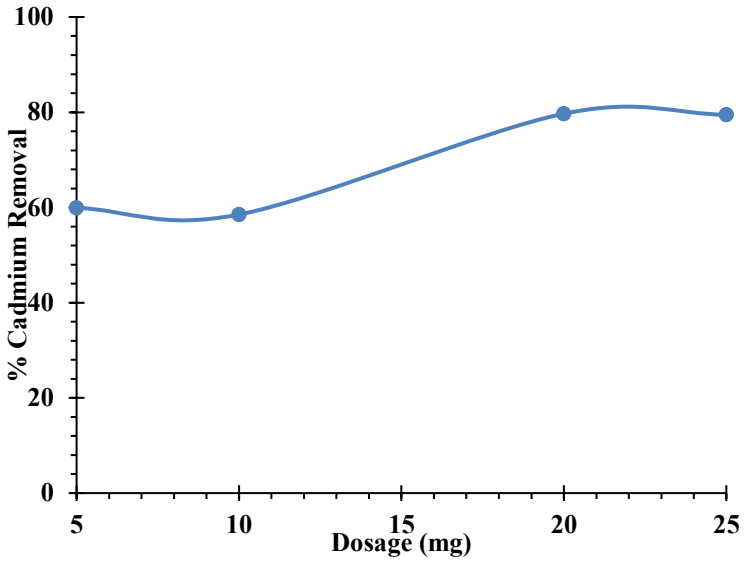

Figure 5.24: Effect of GPHM dosage on cadmium removal (initial cadmium concentration = 0.5 ppm; volume of solution = 50 ml; agitation speed = 200 rpm; initial solution pH = 7; temperature = 298 K; contact time = 30 min)

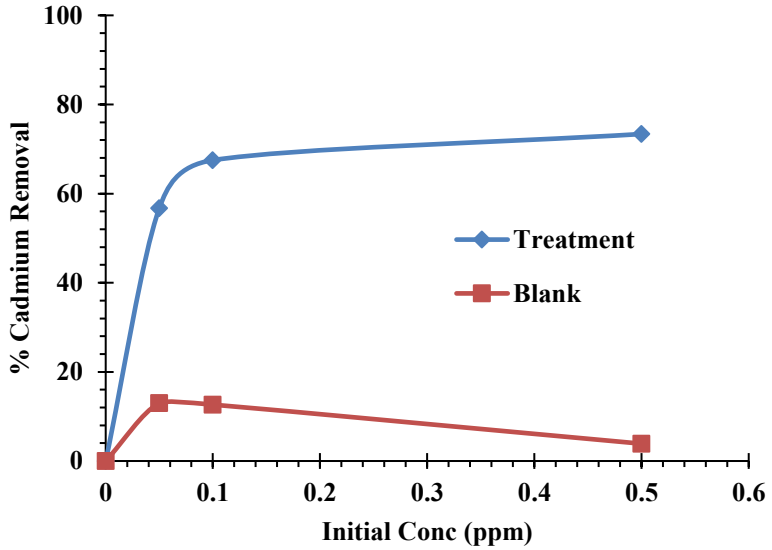

Figure 5.25: Effect of initial concentration of cadmium on its adsorption by GPHM (adsorbent dosage = 25 mg; volume of solution = 50ml; initial solution pH = 7; agitation speed = 200 rpm; temperature = 298 K; contact time = 30 min)

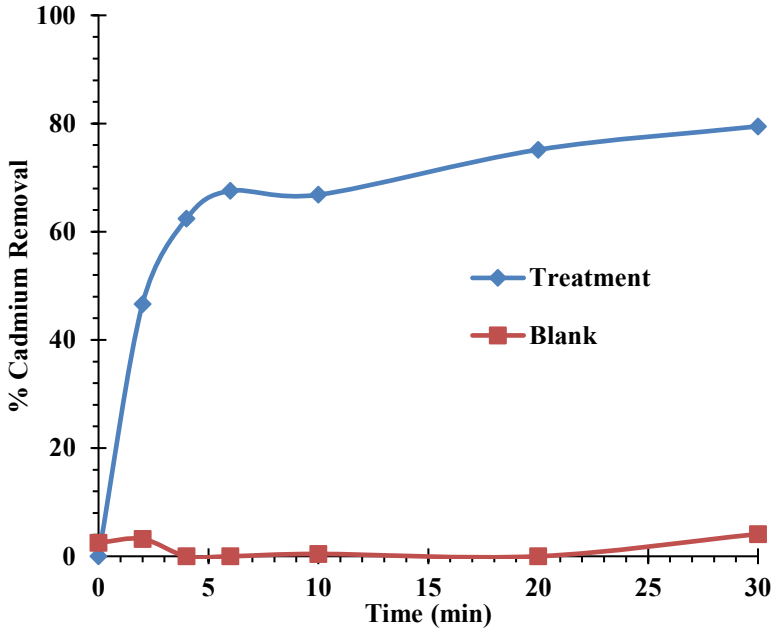

Figure 5.26: Effect of contact time on cadmium adsorption by GPHM (adsorbent dosage = 25 mg; initial cadmium concentration = 0.5 ppm; volume of solution = 50 ml; agitation speed = 200 rpm; initial solution pH = 7; temperature = 298 K)

5.2.3 Kinetics, Isotherms and Thermodynamics

5.2.3.1 Kinetics

Experimental data for kinetic modelling for the adsorption of cadmium by GPHM were obtained under the conditions of adsorbent dosage of 25 mg, initial cadmium aqueous concentration of 0.5 ppm, volume of solution of 50 ml, agitation speed of 200 rpm, initial solution pH 7 and temperature of 298 K. The data were tested by the pseudo-first order and pseudo-second order kinetic models. The results are displayed in Figs. 5.28 and 5.29. From the parameters shown in Table 5.11, the very low R^2 of pseudo-first order is an indication that the adsorption cannot be represented by it. On the other hand, the R^2 of the pseudo-second order model is very high (0.999). Also, its calculated adsorption capacity is almost the same as the one obtained from the experiment. All this indicates that the adsorption of cadmium by GPHM fits into and can be described by the pseudo-second order model. This

can imply that chemical process was probably the one controlling the removal of cadmium from solution by GPHM.

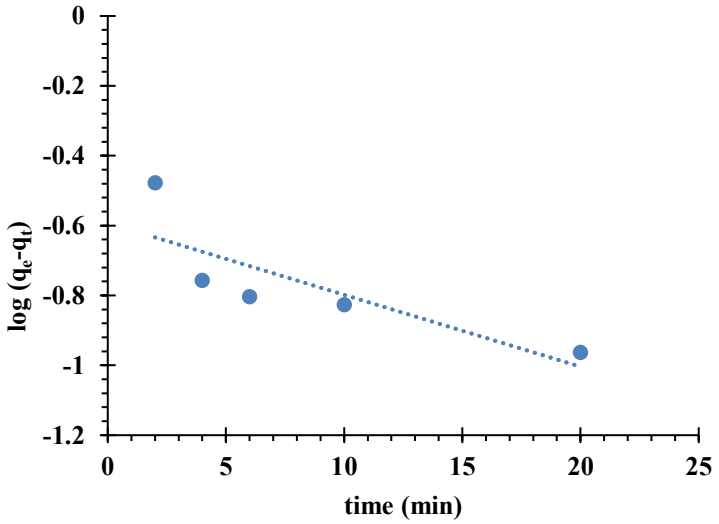

Figure 5.27: Pseudo-first order kinetic plot

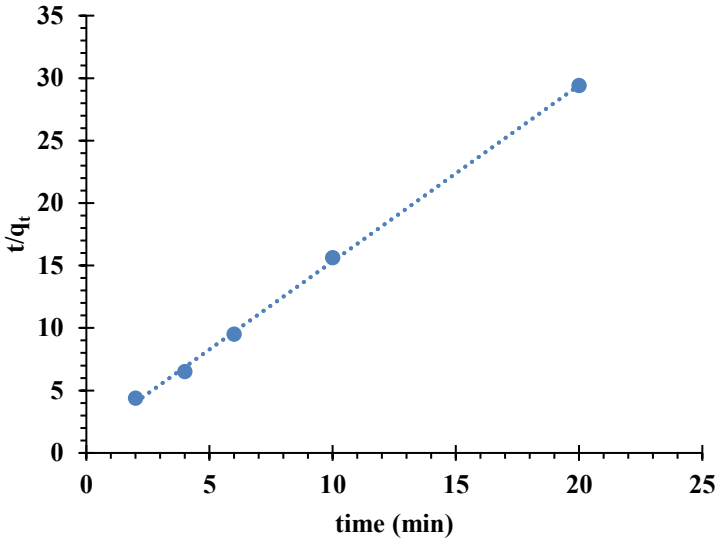

Figure 5.28: Pseudo-second order kinetic plot

Table 5.10: Parameters of kinetic models for the adsorption of cadmium by GPHM

Kinetic model	**Parameters**	**Values**
Pseudo-first-order	q_e (mg/g)	0.256
	k_1 (min^{-1})	0.0474
	R^2	0.675
Pseudo-second-order	q_e (mg/g)	0.709
	k_2 (g/(mg min)	1.605
	R^2	0.999
	q_e experimental (mg/g)	0.789

5.2.3.2 Isotherms Models

The fitness of the experimental data from the cadmium adsorption of GPHM at different initial concentrations of 0.05 ppm, 0.1 ppm and 0.5 ppm were tested on Langmuir, Freundlich and Temkin isotherm models. The plots are shown in Figs 5.30, 5.31 and 5.32 while the parameters are presented in Table 5.12. Assessment of the fitness of the three models based on R^2 revealed that the data fits only Temkin model with R^2 value of 1.00. Thus, the good fit shown by the adsorption experimental data on Temkin model indicates that increase in the surface coverage of GPHM by cadmium ions leads to a linear decrease in the sorption energies. Moreover, the positive value of the constant, b, points to the fact that the adsorption process is exothermic.

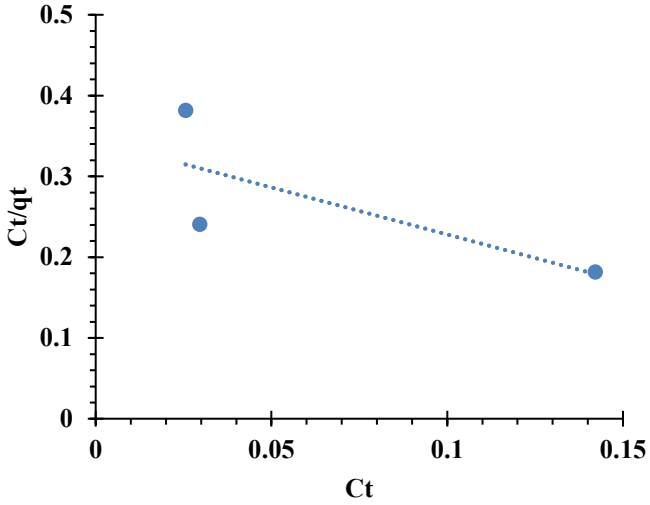

Figure 5.29: Langmuir plot for GPHM

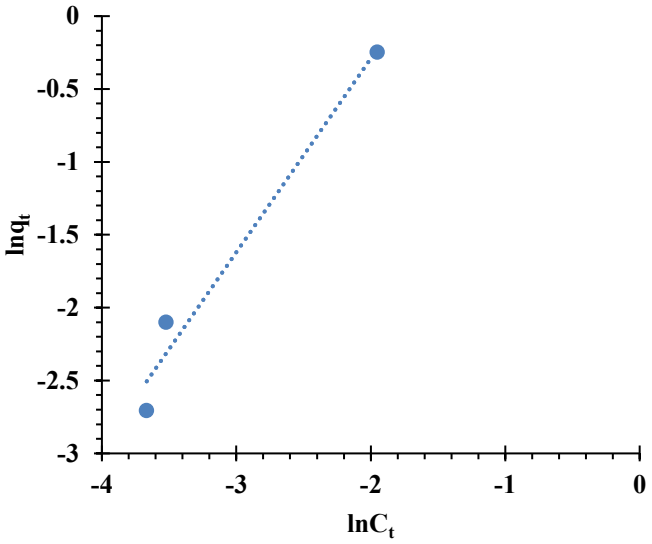

Figure 5.30: Freundlich Plot for GPHM

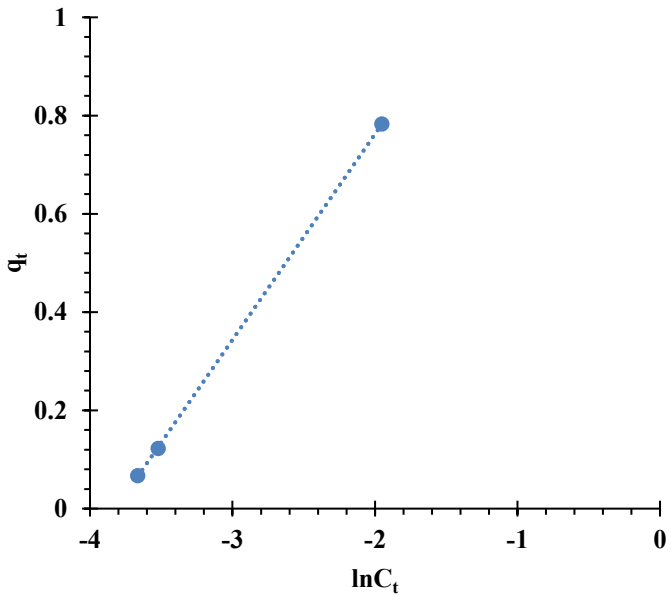

Figure 5.31: Temkin Plot for GPHM

Table 5.11: Parameters of Isotherm models

LANGMUIR	FREUNDLICH	TEMKIN
R^2 = 0.560	R^2 = 0.974	R^2 = 1.000
K_L (L g^{-1}) = 3.380	K_F (mg g^{-1}) = 10.667	K_T (mg g^{-1}) = 45.66
q_m (mg g^{-1}) = 0.859	n = 0.752	b (J mol^{-1}) = 5918.7

5.2.3.3 Thermodynamics

Fig. 5.33 shows the plot of $ln K_o$ versus inverse of absolute temperature and Table 5.13 gives the estimates of the parameters, ΔH, ΔS and ΔG.

A positive ΔH with a magnitude value less than 50 kJ/mol suggests that the adsorption of cadmium by GPHM was endothermic and a physical process. There is also an indication

from the positive value of ΔS that there was an increased disorder at the solid-solution interface.

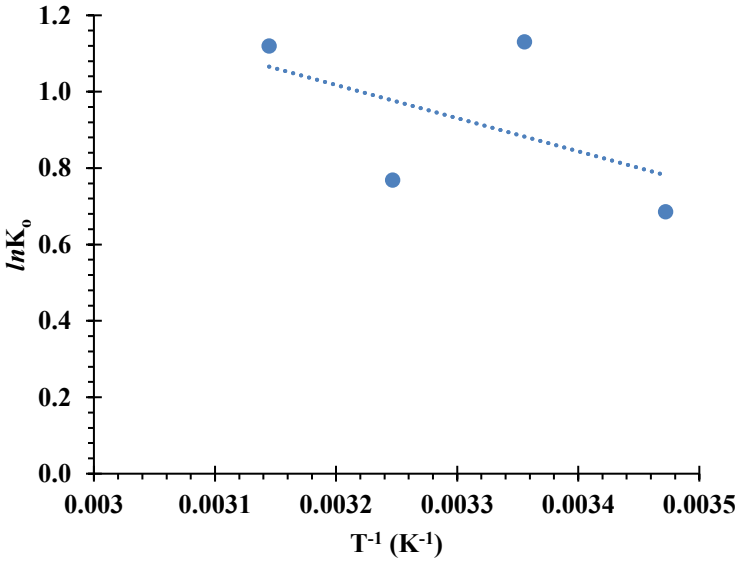

Figure 5.32: Plot of *ln* K_o versus T^{-1} (K^{-1})

Table 5.12: Parameters of thermodynamics

Δ*G* (KJ/mol)				**Δ*H* (KJ/mol)**	**ΔS (J/mol/K)**
288 K	**298 K**	**308 K**	**328 K**	7.217	31.556
-1.642	-2.803	-1.969	-2.962		

Based on the adsorption experimental results, the optimum conditions are initial cadmium concentration of 0.5 ppm, dosage of 20 mg in 50 ml, pH 7, agitation speed of 200 rpm and temperature of 25 ºC. The performance of GPHM for the removal of cadmium as compared to other adsorbents is shown in Table 5.14.

Table 5.13: Comparison of phenol adsorption performance of GPDADMAC with other materials from literature.

Material	Adsorption capacity (mg g^{-1})	% cadmium Removal	Contact Time	Initial cadmium Concentration	Adsorbent dosage	Ref.
Nanocomposite silica aerogel activated carbon	0.384 (Freundlich)	60 %	120 min	20 ml of 3 mg/l	0.1 g	Givianrad et al. (2013) [52]
Activated carbon		50 %	120 min	20 ml of 3 mg/l	0.1 g	
Silica aerogel		30 %	120 min	20 ml of 3 mg/l	0.1 g	
GPHM		60 %	10 min	50 ml of 0.5 mg/l	25 mg	This work

5.2.4 Regeneration Study of GPHM

Fig. 5.34 shows the results obtained from the reuse of regenerated GPHM for the adsorption of cadmium. The adsorption was performed under the conditions of initial cadmium concentration of 2 ppm, GPHM dosage of 100 g in 50 ml, temperature of 298 K, pH value of 7 and agitation speed of 150 rpm. After three cycles of adsorption -desorption, the removal efficiency reduced from about the initial 96 % to about 86 %. This shows that GPHM can be reused at least three times without much change in its removal efficiency of cadmium.

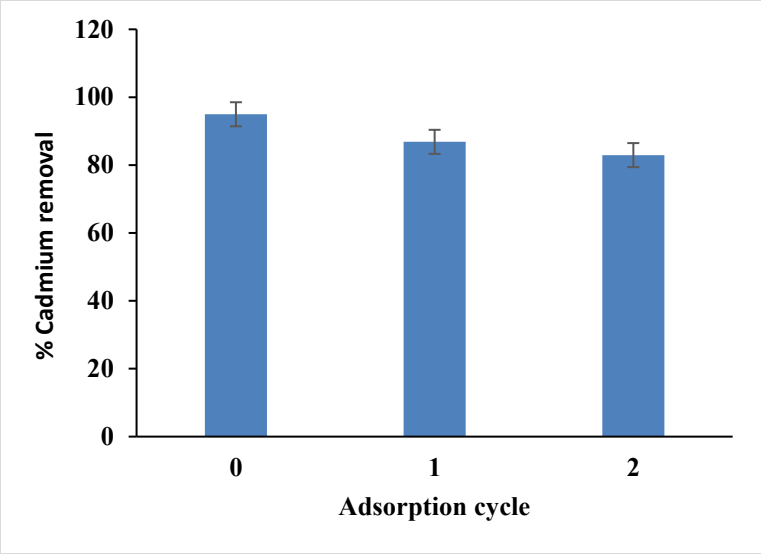

Figure 5.33: Removal efficiency of GPHM for several adsorption/regeneration cycle

5.2.5 Treatment of Cadmium-spiked Groundwater

The effiiciency of GPHM was assessed in the same groundwater sample which was spiked with 2 ppm cadmium. Under the optimum conditions of 100mg adsorbent dosage, volume of 20ml, contact time of 30 min and agitation speed of 200 rpm, the removal efficiency of GPHM was 48% in contrast to the 96% observed in synthetic water. This observation also indicates the interference of the other ions contained in the groundwater sample. They competed with cadmium ions for the available binding sites on GPHM leading to the reduction in the amount of cadmium that can be removed.

CHAPTER 6

CONCLUSIONS AND RECOMMENDATIONS

6.1 CONCLUSIONS

The research has investigated the surface and chemical characteristics as well as the adsorption capacities of graphene-based nanomaterials functionalized differently with two polymeric materials, PDADMAC and PHM. The characterization of GPDADMAC and GPHM was done using techniques such as nitrogen adsorption-desorption, FTIR and SEM/EDX. Based on the nitrogen adsorption isotherms, GPDADMAC has a BET surface area of 357 m^2/g and 198 m^2/g, respectively. The analysis of the FTIR spectrum revealed successful functionalization of the graphene oxides by PDADMAC or PHM. The adsorption treatment was carried out using both synthetic and real groundwater sample. In the synthetic water, GPDADMAC achieved about 80% removal of phenol within 10 min under other parameter conditions of pH of 6, 10 mg/L initial phenol concentration, 4 g/L adsorbent dosage, 298 K temperature and agitation speed of 150 rpm. On the other hand, GPHM was able to attain maximum removal efficiency greater than 60 % for cadmium under the experimental conditions of 0.5 ppm initial cadmium concentration, adsorbent dosage of 25 mg, 50 ml volume of solution, initial solution pH of 7, agitation speed of 200 rpm, contact time of 10 min and temperature of 298 K. Testing of the experimental data on kinetic models showed that the adsorption fitted into the pseudo second order in both cases. This was evidenced by their high coefficients of correlation (>0.99) as well as the closeness of the values of the experimental and calculated adsorption capacities. Also, the experimental data were fitted on isotherm models to gain insight into the mechanisms of

the adsorption processes. The Langmuir and the Temkin isotherm models best described the experimental data for phenol adsorption by GPDADMAC. With regard to cadmium adsorption by GPHM, only the Temkin model fitted the experimental data.

In terms of reusability, the efficiency of GPDADMAC drastically dropped after the first cycle of regeneration. In the case of GPHM, the reusability was still good after the third cycle of regeneration.

The efficiencies of the two materials were tested in real groundwater sample. The groundwater sample was spiked with 10 ppm phenol to assess the efficiency of GPDADMAC while it was spiked with 2 ppm cadmium for the evaluation of the efficiency of GPHM. The removal efficiencies of GPDADMAC and GPHM were 49% and 48%, respectively.

Therefore, this study has shown that the two materials are potentially good adsorbents for fast remediation of water contaminated with phenol and cadmium.

6.2 RECOMMENDATIONS

In line with the outcomes of this research, the following recommendations are suggested for future work:

i. Economic analysis to compare its cost with other materials should be done
ii. The efficiency of the materials at different mixture ratio of polymeric material to graphene would be novel idea.
iii. A further study on the simultaneous removal of phenol and cadmium can be conducted.

iv. The adsorption capacity of the materials for similar organic and trace metal pollutants should be explored.

References

Abbas, A., Al-Amer, A. M., Laoui, T., Al-Marri, M. J., Nasser, M. S., Khraisheh, M., & Atieh, M. A. (2016). Heavy metal removal from aqueous solution by advanced carbon nanotubes: critical review of adsorption applications. *Separation and Purification Technology*, *157*, 141-161.

Abdelwahab, O., & Amin, N. K. (2013). Adsorption of phenol from aqueous solutions by Luffa cylindrica fibers: Kinetics, isotherm and thermodynamic studies. *The Egyptian Journal of Aquatic Research*, *39*(4), 215-223.

Albadarin, A. B., Collins, M. N., Naushad, M., Shirazian, S., Walker, G., & Mangwandi, C. (2017). Activated lignin-chitosan extruded blends for efficient adsorption of methylene blue. *Chemical Engineering Journal*, *307*, 264-272.

Al-Homaidan, A. A., Alabdullatif, J. A., Al-Hazzani, A. A., Al-Ghanayem, A. A., & Alabbad, A. F. (2015). Adsorptive removal of cadmium ions by Spirulina platensis dry biomass. *Saudi journal of biological sciences*, *22*(6), 795-800.

Alinnor, I. J., & Nwachukwu, M. A. (2011). A study on removal characteristics of para-nitrophenol from aqueous solution by fly ash. *Journal of Environmental Chemistry and Ecotoxicology*, *3*(2), 32-36.

Al-Qahtani, K. M. (2017). Cadmium removal from aqueous solution by green synthesis zero valent silver nanoparticles with Benjamina leaves extract. *The Egyptian Journal of Aquatic Research*, *43*(4), 269-274.

Aly, A. A., Hasan, Y. N., & Al-Farraj, A. S. (2014). Olive mill wastewater treatment using a simple zeolite-based low-cost method. *Journal of environmental management*, *145*, 341-348.

Anbia, M., & Ghaffari, A. (2009). Adsorption of phenolic compounds from aqueous solutions using carbon nanoporous adsorbent coated with polymer. *Applied Surface Science*, *255*(23), 9487-9492.

Arshadi, M., Amiri, M. J., & Mousavi, S. (2014). Kinetic, equilibrium and thermodynamic investigations of Ni (II), Cd (II), Cu (II) and Co (II) adsorption on barley straw ash. *Water Resources and Industry*, *6*, 1-17.

Asmaly, H. A., Abussaud, B., Ihsanullah, Saleh, T. A., Bukhari, A. A., Laoui, T., ... & Atieh, M. A. (2015). Evaluation of micro-and nano-carbon-based adsorbents for the removal of phenol from aqueous solutions. *Toxicological & Environmental Chemistry*, *97*(9), 1164-1179.

Asmaly, H. A., Ihsanullah, Abussaud, B., Saleh, T. A., Laoui, T., Gupta, V. K., & Atieh, M. A. (2016). Adsorption of phenol on aluminum oxide impregnated fly ash. *Desalination and Water Treatment*, *57*(15), 6801-6808.

Asmaly, H. A., Saleh, T. A., Laoui, T., Gupta, V. K., & Atieh, M. A. (2015). Enhanced adsorption of phenols from liquids by aluminum oxide/carbon nanotubes: comprehensive study from synthesis to surface properties. *Journal of Molecular Liquids*, *206*, 176-182.

Ayawei, Nimibofa, Augustus Newton Ebelegi, and Donbebe Wankasi. "Modelling and interpretation of adsorption isotherms." *Journal of Chemistry* 2017 (2017).

Bazrafshan, E., Amirian, P., Mahvi, A. H., & Ansari-Moghaddam, A. (2016). Application of adsorption process for phenolic compounds removal from aqueous environments: a systematic review. *Global NEST Journal*, *18*(1), 146-163.

Bian, Y., Bian, Z. Y., Zhang, J. X., Ding, A. Z., Liu, S. L., & Wang, H. (2015). Effect of the oxygen-containing functional group of graphene oxide on the aqueous cadmium ions removal. *Applied Surface Science*, *329*, 269-275.

Biglari, H., Afsharnia, M., Alipour, V., Khosravi, R., Sharafi, K., & Mahvi, A. H. (2017). A review and investigation of the effect of nanophotocatalytic ozonation process for phenolic compound removal from real effluent of pulp and paper industry. *Environmental Science and Pollution Research*, *24*(4), 4105-4116.

Bohli, T., Ouederni, A., Fiol, N., & Villaescusa, I. (2015). Evaluation of an activated carbon from olive stones used as an adsorbent for heavy metal removal from aqueous phases. *Comptes rendus chimie*, *18*(1), 88-99.

Bolto, B., & Gregory, J. (2007). Organic polyelectrolytes in water treatment. *Water research*, *41*(11), 2301-2324.

Burakov, A. E., Galunin, E. V., Burakova, I. V., Kucherova, A. E., Agarwal, S., Tkachev, A. G., & Gupta, V. K. (2018). Adsorption of heavy metals on conventional and nanostructured materials for wastewater treatment purposes: A review. *Ecotoxicology and environmental safety*, *148*, 702-712.

Busca, G., Berardinelli, S., Resini, C., & Arrighi, L. (2008). Technologies for the removal of phenol from fluid streams: a short review of recent developments. *Journal of Hazardous Materials*, *160*(2-3), 265-288.

Cai, D., & Song, M. (2010). Recent advance in functionalized graphene/polymer nanocomposites. *Journal of Materials Chemistry*, *20*(37), 7906-7915.

Carolin, C. F., Kumar, P. S., Saravanan, A., Joshiba, G. J., & Naushad, M. (2017). Efficient techniques for the removal of toxic heavy metals from aquatic environment: A review. *Journal of Environmental Chemical Engineering*, *5*(3), 2782-2799.

Chabicovsky, M., Klepal, W., & Dallinger, R. (2004). Mechanisms of cadmium toxicity in terrestrial pulmonates: programmed cell death and metallothionein overload. *Environmental Toxicology and Chemistry: An International Journal*, *23*(3), 648-655.

Chowdhury, S., & Balasubramanian, R. (2014). Recent advances in the use of graphene-family nanoadsorbents for removal of toxic pollutants from wastewater. *Advances in colloid and interface science*, *204*, 35-56.

Coates, J. (2000). Interpretation of infrared spectra, a practical approach. *Encyclopedia of analytical chemistry*, *12*, 10815-10837.

Cui, Y., Liu, X. Y., Chung, T. S., Weber, M., Staudt, C., & Maletzko, C. (2016). Removal of organic micro-pollutants (phenol, aniline and nitrobenzene) via forward osmosis (FO) process: evaluation of FO as an alternative method to reverse osmosis (RO). *Water research*, *91*, 104-114.

De Gisi, S., Lofrano, G., Grassi, M., & Notarnicola, M. (2016). Characteristics and adsorption capacities of low-cost sorbents for wastewater treatment: a review. *Sustainable Materials and Technologies*, *9*, 10-40.

Ding, L., Liu, Y., Guo, S. X., Zhai, J., Bond, A. M., & Zhang, J. (2014). Phosphomolybdate@ poly (diallyldimethylammonium chloride)-reduced graphene oxide modified electrode for highly efficient electrocatalytic reduction of bromate. *Journal of Electroanalytical Chemistry*, *727*, 69-77.

Dolaksiz, Y. E., Temel, F., & Tabakci, M. (2018). Adsorption of phenolic compounds onto calix [4] arene-bonded silica gels from aqueous solutions. *Reactive and Functional Polymers*, *126*, 27-35.

Edwards, R. S., & Coleman, K. S. (2013). Graphene synthesis: relationship to applications. *Nanoscale*, *5*(1), 38-51.

Ehrampoush, M. H., Miria, M., Salmani, M. H., & Mahvi, A. H. (2015). Cadmium removal from aqueous solution by green synthesis iron oxide nanoparticles with tangerine peel extract. *Journal of Environmental Health Science and Engineering*, *13*(1), 84.

El Maghraby, M. M., El Nasr, A. K. O. A., & Hamouda, M. S. (2013). Quality assessment of groundwater at south Al Madinah Al Munawarah area, Saudi Arabia. *Environmental earth sciences*, *70*(4), 1525-1538.

Fajardo, A. S., Rodrigues, R. F., Martins, R. C., Castro, L. M., & Quinta-Ferreira, R. M. (2015). Phenolic wastewaters treatment by electrocoagulation process using Zn anode. *Chemical Engineering Journal*, *275*, 331-341.

Fang, M., Wang, K., Lu, H., Yang, Y., & Nutt, S. (2009). Covalent polymer functionalization of graphene nanosheets and mechanical properties of composites. *Journal of Materials Chemistry*, *19*(38), 7098-7105.

Faroon, O., Ashizawa, A., Wright, S., Tucker, P., Jenkins, K., Ingerman, L., & Rudisill, C. (2012). Toxicological Profile for Cadmium, Agency for Toxic Substances and Disease Registry (ATSDR) Toxicological Profiles. *Agency for Toxic Substances and Disease Registry (US), Atlanta (GA)*.

Faust, S. D., & Aly, O. M. (2013). *Adsorption processes for water treatment*. Elsevier.

Friberg, Lars. Cadmium in the Environment: 0. CRC press, 2017.

Gautam, R. K., Mudhoo, A., Lofrano, G., & Chattopadhyaya, M. C. (2014). Biomass-derived biosorbents for metal ions sequestration: Adsorbent modification and activation methods and adsorbent regeneration. *Journal of environmental chemical engineering*, *2*(1), 239-259.

Georgakilas, V., Otyepka, M., Bourlinos, A. B., Chandra, V., Kim, N., Kemp, K. C., ... & Kim, K. S. (2012). Functionalization of graphene: covalent and non-covalent approaches, derivatives and applications. *Chemical reviews, 112(11)*, 6156-6214.

Gong, Z., Li, S., Han, W., Wang, J., Ma, J., & Zhang, X. (2016). Recyclable graphene oxide grafted with poly (N-isopropylacrylamide) and its enhanced selective adsorption for phenols. *Applied Surface Science*, *362*, 459-468.

Gupta, V. K., Kumar, R., Nayak, A., Saleh, T. A., & Barakat, M. A. (2013). Adsorptive removal of dyes from aqueous solution onto carbon nanotubes: a review. *Advances in colloid and interface science*, *193*, 24-34.

Hosseinabadi-Farahani, Z., Hosseini-Monfared, H., & Mahmoodi, N. M. (2015). Graphene oxide nanosheet: preparation and dye removal from binary system colored wastewater. *Desalination and Water Treatment*, *56*(9), 2382-2394.

Hu, R., Dai, S., Shao, D., Alsaedi, A., Ahmad, B., & Wang, X. (2015). Efficient removal of phenol and aniline from aqueous solutions using graphene oxide/polypyrrole composites. *Journal of Molecular Liquids*, *203*, 80-89.

Hu, X. J., Liu, Y. G., Zeng, G. M., Wang, H., Hu, X., Chen, A. W., ... & Liu, S. H. (2014). Effect of aniline on cadmium adsorption by sulfanilic acid-grafted magnetic graphene oxide sheets. *Journal of colloid and interface science*, *426*, 213-220.

Huang, M., Xu, X., Yang, H., & Liu, S. (2012). Electrochemically-driven and dynamic enhancement of drug metabolism via cytochrome P450 microsomes on colloidal gold/graphene nanocomposites. *RSC Advances*, *2*(33), 12844-12850.

Indrawirawan, S., Sun, H., Duan, X., & Wang, S. (2015). Nanocarbons in different structural dimensions (0–3D) for phenol adsorption and metal-free catalytic oxidation. *Applied Catalysis B: Environmental*, *179*, 352-362.

Inyinbor, A. A., Adekola, F. A., & Olatunji, G. A. (2016). Kinetics, isotherms and thermodynamic modeling of liquid phase adsorption of Rhodamine B dye onto Raphia hookerie fruit epicarp. *Water Resources and Industry*, *15*, 14-27.

Izah, S. C., Chakrabarty, N., & Srivastav, A. L. (2016). A review on heavy metal concentration in potable water sources in Nigeria: Human health effects and mitigating measures. *Exposure and Health*, *8*(2), 285-304.

Ji, L., Chen, W., Xu, Z., Zheng, S., & Zhu, D. (2013). Graphene nanosheets and graphite oxide as promising adsorbents for removal of organic contaminants from aqueous solution. *Journal of environmental quality*, *42*(1), 191-198.

Kharismadewi, D., Haldorai, Y., Nguyen, V. H., Tuma, D., & Shim, J. J. (2016). Synthesis of graphene oxide-poly (2-hydroxyethyl methacrylate) composite by dispersion polymerization in supercritical CO2: adsorption behavior for the removal of organic dye. *Composite Interfaces*, *23*(7), 719-739.

Kuila, T., Bose, S., Mishra, A. K., Khanra, P., Kim, N. H., & Lee, J. H. (2012). Chemical functionalization of graphene and its applications. *Progress in Materials Science*, *57*(7), 1061-1105.

Larsen, T. A., Hoffmann, S., Lüthi, C., Truffer, B., & Maurer, M. (2016). Emerging solutions to the water challenges of an urbanizing world. *Science*, *352*(6288), 928-933.Kim, Sewoon, et al. "Aqueous removal of inorganic and organic contaminants by graphene-based nanoadsorbents: A review." *Chemosphere* 212 (2018): 1104-1124.

Li, H., Jia, L. P., Ma, R. N., Jia, W. L., & Wang, H. S. (2017). Electrodeposition of PtNPs on the LBL assembled multilayer films of (PDDA-GS/PEDOT: PSS) n and their electrocatalytic activity toward methanol oxidation. *RSC Advances*, *7*(27), 16371-16378.

Li, H., Sheng, K., Xie, Z., Zou, L., & Ye, B. (2016). Highly sensitive determination of hyperin on poly (diallyldimethylammonium chloride)-functionalized graphene modified electrode. *Journal of Electroanalytical Chemistry*, *776*, 105-113.

Li, J., Chen, C., Zhu, K., & Wang, X. (2016). Nanoscale zero-valent iron particles modified on reduced graphene oxides using a plasma technique for Cd (II) removal. *Journal of the Taiwan Institute of Chemical Engineers*, *59*, 389-394.

Li, Y., Du, Q., Liu, T., Sun, J., Jiao, Y., Xia, Y., ... & Zhu, H. (2012). Equilibrium, kinetic and thermodynamic studies on the adsorption of phenol onto graphene. *Materials Research Bulletin*, *47*(8), 1898-1904.

Liadi, M. A., Tawabini, B., Shawabkeh, R., Jarrah, N., Oyehan, T. A., Shaibani, A., & Makkawi, M. (2018). Treating MTBE-contaminated water using sewage sludge-derived activated carbon. *Environmental Science and Pollution Research*, *25*(29), 29397-29407.

Liu, C., Han, K., Lee, D. J., & Wang, Q. (2016). Simultaneous biological removal of phenol, sulfide, and nitrate using expanded granular sludge bed reactor. *Applied microbiology and biotechnology*, *100*(9), 4211-4217.

Liu, C., Zhang, D., Zhao, L., Lu, X., Zhang, P., He, S., ... & Tang, X. (2016). Synthesis of a thiacalix [4] arenetetrasulfonate-functionalized reduced graphene oxide adsorbent for the removal of lead (II) and cadmium (II) from aqueous solutions. *RSC Advances*, *6*(114), 113352-113365.

Liu, F. Q., Xia, M. F., Yao, S. L., Li, A. M., Wu, H. S., & Chen, J. L. (2008). Adsorption equilibria and kinetics for phenol and cresol onto polymeric adsorbents: Effects of adsorbents/adsorbates structure and interface. *Journal of hazardous materials*, *152*(2), 715-720.

Liu, J., Xie, J., Ren, Z., & Zhang, W. (2013). Solvent extraction of phenol with cumene from wastewater. *Desalination and Water Treatment*, *51*(19-21), 3826-3831.

Liu, P. R., Zhang, H. L., Wang, T., Yang, W. L., Hong, Y., & Hou, Y. L. (2016). Functional graphene-based magnetic nanocomposites as magnetic flocculant for efficient harvesting of oleaginous microalgae. *Algal Research*, *19*, 86-95.

Liu, Z., Zhu, S., Li, Y., Li, Y., Shi, P., Huang, Z., & Huang, X. (2015). Preparation of graphene/poly (2-hydroxyethyl acrylate) nanohybrid materials via an ambient temperature "grafting-from" strategy. *Polymer Chemistry*, *6*(2), 311-321.

Luo, X., Wang, C., Wang, L., Deng, F., Luo, S., Tu, X., & Au, C. (2013). Nanocomposites of graphene oxide-hydrated zirconium oxide for simultaneous removal of As (III) and As (V) from water. *Chemical engineering journal*, *220*, 98-106.

Malik, D. S., Jain, C. K., & Yadav, A. K. (2017). Removal of heavy metals from emerging cellulosic low-cost adsorbents: a review. *Applied water science*, *7*(5), 2113-2136.

Massoumi, B., Ghandomi, F., Abbasian, M., Eskandani, M., & Jaymand, M. (2016). Surface functionalization of graphene oxide with poly (2-hydroxyethyl methacrylate)-graft-poly (ε-caprolactone) and its electrospun nanofibers with gelatin. *Applied Physics A*, *122*(12), 1000.

Meniai, A. H. (2012). The use of sawdust as by product adsorbent of organic pollutant from wastewater: adsorption of phenol. *Energy Procedia*, *18*, 905-914.

Mittal, G., Dhand, V., Rhee, K. Y., Park, S. J., & Lee, W. R. (2015). A review on carbon nanotubes and graphene as fillers in reinforced polymer nanocomposites. *Journal of Industrial and Engineering Chemistry*, *21*, 11-25.

Mohammadi, S., Kargari, A., Sanaeepur, H., Abbassian, K., Najafi, A., & Mofarrah, E. (2015). Phenol removal from industrial wastewaters: a short review. *Desalination and Water Treatment*, *53*(8), 2215-2234.

Mohanty, K., Das, D., & Biswas, M. N. (2005). Adsorption of phenol from aqueous solutions using activated carbons prepared from Tectona grandis sawdust by ZnCl2 activation. *Chemical Engineering Journal*, *115*(1-2), 121-131.

Mousset, E., Frunzo, L., Esposito, G., Van Hullebusch, E. D., Oturan, N., & Oturan, M. A. (2016). A complete phenol oxidation pathway obtained during electro-Fenton treatment and validated by a kinetic model study. *Applied Catalysis B: Environmental*, *180*, 189-198.

Mukherjee, M., Goswami, S., Banerjee, P., Sengupta, S., Das, P., Banerjee, P. K., & Datta, S. (2017). Ultrasonic assisted graphene oxide nanosheet for the removal of phenol containing solution. *Environmental Technology & Innovation*.

Nguyen, M. L., Huang, C., & Juang, R. S. (2016). Synergistic biosorption between phenol and nickel (II) from Binary mixtures on chemically and biologically modified chitosan beads. *Chemical Engineering Journal*, *286*, 68-75.

Olabemiwo, F. A., Tawabini, B. S., Patel, F., Oyehan, T. A., Khaled, M., & Laoui, T. (2017). Cadmium Removal from Contaminated Water Using Polyelectrolyte-Coated Industrial Waste Fly Ash. *Bioinorganic chemistry and applications*, *2017*.

Park, J., & Yan, M. (2012). Covalent functionalization of graphene with reactive intermediates. *Accounts of chemical research*, *46*(1), 181-189.

Pavoski, G., Maraschin, T., Milani, M. A., Azambuja, D. S., Quijada, R., Moura, C. S., ... & Galland, G. B. (2015). Polyethylene/reduced graphite oxide nanocomposites with improved morphology and conductivity. *Polymer*, *81*, 79-86.

Peng, W., Li, H., Liu, Y., & Song, S. (2017). A review on heavy metal ions adsorption from water by graphene oxide and its composites. *Journal of Molecular Liquids*, *230*, 496-504.

Perreault, F., De Faria, A. F., & Elimelech, M. (2015). Environmental applications of graphene-based nanomaterials. *Chemical Society Reviews*, *44*(16), 5861-5896.

Pham, T. H., Lee, B. K., & Kim, J. (2016). Improved adsorption properties of a nano zeolite adsorbent toward toxic nitrophenols. *Process Safety and Environmental Protection*, *104*, 314-322.

Pradeep, N. V., Anupama, S., Navya, K., Shalini, H. N., Idris, M., & Hampannavar, U. S. (2015). Biological removal of phenol from wastewaters: a mini review. *Applied Water Science*, *5*(2), 105-112.

Punetha, V. D., Rana, S., Yoo, H. J., Chaurasia, A., McLeskey Jr, J. T., Ramasamy, M. S., ... & Cho, J. W. (2017). Functionalization of carbon nanomaterials for advanced polymer nanocomposites: A comparison study between CNT and graphene. *Progress in Polymer Science*, *67*, 1-47.

Rehman, Z. U., Khan, S., Brusseau, M. L., & Shah, M. T. (2017). Lead and cadmium contamination and exposure risk assessment via consumption of vegetables grown in agricultural soils of five-selected regions of Pakistan. *Chemosphere*, *168*, 1589-1596.

Roig, B., Gonzalez, C., & Thomas, O. (2003). Monitoring of phenol photodegradation by ultraviolet spectroscopy. *Spectrochimica Acta Part A: Molecular and Biomolecular Spectroscopy*, *59*(2), 303-307.

Rouquerol, J., Rouquerol, F., Llewellyn, P., Maurin, G., & Sing, K. S. (2013). *Adsorption by powders and porous solids: principles, methodology and applications*. Academic press.

Saleh, T. A. (2016). Nanocomposite of carbon nanotubes/silica nanoparticles and their use for adsorption of Pb (II): from surface properties to sorption mechanism. *Desalination and Water Treatment*, *57*(23), 10730-10744.

Saleh, T. A., Sarı, A., & Tuzen, M. (2017). Effective adsorption of antimony (III) from aqueous solutions by polyamide-graphene composite as a novel adsorbent. *Chemical Engineering Journal*, *307*, 230-238.

Saleh, T. A., Tuzen, M., & Sarı, A. (2017). Magnetic activated carbon loaded with tungsten oxide nanoparticles for aluminum removal from waters. *Journal of Environmental Chemical Engineering*, *5*(3), 2853-2860.

Sharaf, M. A. M., & Subyani, A. M. (2011). Assessing of groundwater contamination by toxic elements through multivariate statistics and spatial interpolation, Wadi Fatimah, Western Arabian Shield, Saudi Arabia. *Int. J. of Sci. & Eng. Res*, *2*(9).

Sheka, E. F. (2014). The uniqueness of physical and chemical natures of graphene: their coherence and conflicts. *International Journal of Quantum Chemistry*, *114*(16), 1079-1095.

Sherlala, A. I. A., Raman, A. A. A., Bello, M. M., & Asghar, A. (2018). A review of the applications of organo-functionalized magnetic graphene oxide nanocomposites for heavy metal adsorption. *Chemosphere*, *193*, 1004-1017.

Shet, A., & Vidya, S. K. (2016). Solar light mediated photocatalytic degradation of phenol using Ag core–TiO2 shell (Ag@ TiO2) nanoparticles in batch and fluidized bed reactor. *Solar Energy*, *127*, 67-78.

Şinoforoğlu, M., Gür, B., Arık, M., Onganer, Y., & Meral, K. (2013). Graphene oxide sheets as a template for dye assembly: graphene oxide sheets induce H-aggregates of pyronin (Y) dye. *Rsc Advances*, *3*(29), 11832-11838.

Sitko, R., Turek, E., Zawisza, B., Malicka, E., Talik, E., Heimann, J., ... & Wrzalik, R. (2013). Adsorption of divalent metal ions from aqueous solutions using graphene oxide. *Dalton transactions*, *42*(16), 5682-5689.

Smets, K., De Jong, M., Lupul, I., Gryglewicz, G., Schreurs, S., Carleer, R., & Yperman, J. (2016). Rapeseed and raspberry seed cakes as inexpensive raw materials in the production of activated carbon by physical activation: effect of activation conditions on textural and phenol adsorption characteristics. *Materials*, *9*(7), 565.

Soleimani, K., Tehrani, A. D., & Adeli, M. (2018). Bioconjugated graphene oxide hydrogel as an effective adsorbent for cationic dyes removal. *Ecotoxicology and environmental safety*, *147*, 34-42.

Sousa, J. C., Ribeiro, A. R., Barbosa, M. O., Pereira, M. F. R., & Silva, A. M. (2018). A review on environmental monitoring of water organic pollutants identified by EU guidelines. *Journal of hazardous materials*, *344*, 146-162.

Srivastava, S. K., Tyagi, R., Pal, N., & Mohan, D. (1997). Process development for removal of substituted phenol by carbonaceous adsorbent obtained from fertilizer waste. *Journal of Environmental Engineering*, *123*(9), 842-851.

Tan, P., Sun, J., Hu, Y., Fang, Z., Bi, Q., Chen, Y., & Cheng, J. (2015). Adsorption of Cu^{2+}, Cd^{2+} and Ni^{2+} from aqueous single metal solutions on graphene oxide membranes. *Journal of hazardous materials*, *297*, 251-260.

Thines, R. K., Mubarak, N. M., Nizamuddin, S., Sahu, J. N., Abdullah, E. C., & Ganesan, P. (2017). Application potential of carbon nanomaterials in water and wastewater treatment: a review. *Journal of the Taiwan Institute of Chemical Engineers*, *72*, 116-133.

Thirumavalavan, M., Lai, Y. L., Lin, L. C., & Lee, J. F. (2009). Cellulose-based native and surface modified fruit peels for the adsorption of heavy metal ions from aqueous solution: Langmuir adsorption isotherms. *Journal of Chemical & Engineering Data*, *55*(3), 1186-1192.

Thue, P. S., Sophia, A. C., Lima, E. C., Wamba, A. G., de Alencar, W. S., dos Reis, G. S., ... & Dias, S. L. (2018). Synthesis and characterization of a novel organic-inorganic hybrid clay adsorbent for the removal of acid red 1 and acid green 25 from aqueous solutions. *Journal of Cleaner Production*, *171*, 30-44.

Tripathi, A., & Ranjan, M. R. (2015). Heavy metal removal from wastewater using low cost adsorbents. *J Bioremed Biodeg*, *6*(1000315), 5.

Ţucureanu, V., Matei, A., & Avram, A. M. (2016). FTIR spectroscopy for carbon family study. *Critical reviews in analytical chemistry*, *46*(6), 502-520.

Upadhyay, R. K., Soin, N., & Roy, S. S. (2014). Role of graphene/metal oxide composites as photocatalysts, adsorbents and disinfectants in water treatment: a review. *Rsc Advances*, *4*(8), 3823-3851.

Víctor-Ortega, M. D., Ochando-Pulido, J. M., & Martínez-Ferez, A. (2016). Performance and modeling of continuous ion exchange processes for phenols recovery from olive mill wastewater. *Process Safety and Environmental Protection*, *100*, 242-251.

Villegas, L. G. C., Mashhadi, N., Chen, M., Mukherjee, D., Taylor, K. E., & Biswas, N. (2016). A short review of techniques for phenol removal from wastewater. *Current Pollution Reports*, *2*(3), 157-167.

Wang, J., & Chen, B. (2015). Adsorption and coadsorption of organic pollutants and a heavy metal by graphene oxide and reduced graphene materials. *Chemical Engineering Journal*, *281*, 379-388.

Wang, X., Liu, B., Lu, Q., & Qu, Q. (2014). Graphene-based materials: Fabrication and application for adsorption in analytical chemistry. *Journal of Chromatography A*, *1362*, 1-15.

Wang, X., Lu, M., Wang, H., Pei, Y., Rao, H., & Du, X. (2015). Three-dimensional graphene aerogels–mesoporous silica frameworks for superior adsorption capability of phenols. *Separation and Purification Technology*, *153*, 7-13.

Wu, S., Zhang, K., Wang, X., Jia, Y., Sun, B., Luo, T., ... & Kong, L. (2015). Enhanced adsorption of cadmium ions by 3D sulfonated reduced graphene oxide. *Chemical Engineering Journal*, *262*, 1292-1302.

Xin, G., Yao, T., Sun, H., Scott, S. M., Shao, D., Wang, G., & Lian, J. (2015). Highly thermally conductive and mechanically strong graphene fibers. *Science*, *349*(6252), 1083-1087.

Yang, D. Q., Rochette, J. F., & Sacher, E. (2005). Spectroscopic evidence for π− π interaction between poly (diallyl dimethylammonium) chloride and multiwalled carbon nanotubes. *The Journal of Physical Chemistry B*, *109*(10), 4481-4484.

Yari, M., Rajabi, M., Moradi, O., Yari, A., Asif, M., Agarwal, S., & Gupta, V. K. (2015). Kinetics of the adsorption of Pb (II) ions from aqueous solutions by graphene oxide and thiol functionalized graphene oxide. *Journal of Molecular Liquids*, *209*, 50-57.

Yu, J. G., Yu, L. Y., Yang, H., Liu, Q., Chen, X. H., Jiang, X. Y., ... & Jiao, F. P. (2015). Graphene nanosheets as novel adsorbents in adsorption, preconcentration and

removal of gases, organic compounds and metal ions. *Science of the total environment*, *502*, 70-79.

Yu, S., Wang, X., Yao, W., Wang, J., Ji, Y., Ai, Y., ... & Wang, X. (2017). Macroscopic, spectroscopic, and theoretical investigation for the interaction of phenol and naphthol on reduced graphene oxide. *Environmental science & technology*, *51*(6), 3278-3286.

Zare, K., Gupta, V. K., Moradi, O., Makhlouf, A. S. H., Sillanpää, M., Nadagouda, M. N., ... & Tyagi, I. (2015). A comparative study on the basis of adsorption capacity between CNTs and activated carbon as adsorbents for removal of noxious synthetic dyes: a review. *Journal of nanostructure in chemistry*, *5*(2), 227-236.

Zeng, S., Gan, N., Weideman-Mera, R., Cao, Y., Li, T., & Sang, W. (2013). Enrichment of polychlorinated biphenyl 28 from aqueous solutions using Fe3O4 grafted graphene oxide. *Chemical engineering journal*, *218*, 108-115.

Zhang, Y., Peng, W., Xia, L., & Song, S. (2017). Adsorption of Cd (II) at the Interface of water and graphene oxide prepared from flaky graphite and amorphous graphite. *Journal of Environmental Chemical Engineering*, *5*(4), 4157-4164.

Zhang, Y., Shao, D., Yan, J., Jia, X., Li, Y., Yu, P., & Zhang, T. (2016). The pore size distribution and its relationship with shale gas capacity in organic-rich mudstone of Wufeng-Longmaxi Formations, Sichuan Basin, China. *Journal of Natural Gas Geoscience*, *1*(3), 213-220.

Zhao, G., Li, J., Ren, X., Chen, C., & Wang, X. (2011). Few-layered graphene oxide nanosheets as superior sorbents for heavy metal ion pollution management. *Environmental science & technology*, *45*(24), 10454-10462.

Zhu, Y., Murali, S., Cai, W., Li, X., Suk, J. W., Potts, J. R., & Ruoff, R. S. (2010). Graphene and graphene oxide: synthesis, properties, and applications. *Advanced materials*, *22*(35), 3906-3924.

Vitae

Personal Details

Name : Abideen Ojo Salawudeen

Nationality : Nigeria

Date of Birth : April 17, 1986

Email : salabid09@gmail.com

Address : 59, Ire-Akari Zone, Olunloyo-Akanran, Ibadan, Oyo State, Postal Code 200242, Nigeria

Academic Background

- MSc. Environmental Sciences, May 2019.

  King Fahd University of Petroleum and Minerals, Dhahran, Saudi Arabia.

  MSc. Thesis Title: Removal of phenol and cadmium from contaminated water by polymeric modified graphene nanomaterials.

- B. Agric. (Agricultural Economics), November 2009.

  University of Ibadan, Nigeria.

  Project Title: Effects of social capital on the food security status of residents of Ona-Ara Local Government Area, Nigeria.

Academic and Research Experiences

Teaching Assistant of Environmental Chemistry 2018

King Fahd University of Petroleum & Minerals

Teaching Assistant of Sustaining the Earth 2018

King Fahd University of Petroleum & Minerals

Publications

Salawudeen A.O., Tawabini B.S., Saleh T.A & Al-Shaibani A.M., Evaluation of the removal of phenol from contaminated water by graphene oxide functionalized with poly dially dimethyl ammonium chloride (GPDADMAC). *Desalination and Water Treatment r Journal*. (TDWT-2018-2058.R1) (under review).

Abideen O. Salawudeen, Bassam S. Tawabini, Abdulaziz M. Al-Shaibani & Tawfik A. Saleh, Evaluation of the removal of cadmium from contaminated water by graphene oxide functionalized with polymer based 2-hydroxyethyl methacrylate (GPHM). *Journal of molecular Liquids, MOLLIQ_2019_717* (under review).

Bassam S. Tawabini, Tawfik A. Saleh, Abdulaziz M. Al-Shaibani & Abideen O. Salawudeen. A review on adsorption of cadmium by modified and unmodified graphene. (prepared manuscript)

Conference Presentation

Salawudeen A.O., Tawabini B.S., Saleh T.A & Al-Shaibani A.M. (19th Feb, 2019), Evaluation of the removal of phenol from contaminated water by graphene oxide functionalized with poly dially dimethyl ammonium chloride (GPDADMAC), *Petro-Environment.*